

**RAPID CHARACTERIZATION OF POOR-QUALITY MEDICINES USING
MASS SPECTROMETRY**

A Thesis
Presented to
The Academic Faculty

By

David Vincent Donndelinger

In Partial Fulfillment
Of the Requirements for the Degree
Master of Science in Chemistry

Georgia Institute of Technology

December 2018

Copyright © 2018 by David V. Donndelinger

**RAPID CHARACTERIZATION OF POOR-QUALITY MEDICINES USING
MASS SPECTROMETRY**

Approved by:

Dr. Facundo M. Fernández, Advisor
School of Chemistry and Biochemistry
Georgia Institute of Technology

Dr. Ronghu Wu
School of Chemistry and Biochemistry
Georgia Institute of Technology

Dr. Amanda Stockton
School of Chemistry and Biochemistry
Georgia Institute of Technology

Date Approved: November 16, 2018

DEDICATION

This thesis is dedicated to my wife and son. Genevieve, you have been an inspiration for me. You are my joy, energy, and better half. Everything I do, I do it for our family in support of our calling to glorify God in all things. To my son, William, may you always serve the Lord our God throughout your entire life. May you always investigate and learn, stand firm on the foundation, and be captivated with all of creation. Soli Deo Gloria.

ACKNOWLEDGEMENTS

I am thoroughly grateful to Dr. Fernandez. He took me into his group when no one else wanted a master's student. He has continuously supported my family through numerous issues during this time; he always encouraged me and gave me time to take care of my family. I thank him for his unending help with research and his gracious understanding with my family. I thank the other professors on my committee, Dr. Ronghu Wu and Dr. Amanda Stockton, for their expertise and assistance in this effort.

I thank the United States Air Force for fully funding this degree. They have granted me an outstanding career in the greatest military in the history of the world.

Stephen Zambrzycki was an immense help to this project. I would not be graduating with a thesis had it not been for him. I thank him for his tireless efforts, long nights, and always answering my endless questions.

I am immensely thankful to my parents, Vincent and Denise Donndelinger. My mom has always given me her energy, and wise perspective. My father always taught me that the love of science and the love of God are not opposed to each other but rather they are one in the same. He fueled me with his deep knowledge and immense ability to think critically. Their constant prayer and encouragement were foundational to this work.

With all my heart, I thank my wife, Genevieve. She has endured multiple life changing events, constant medical issues, challenging circumstances, and yet through it all she is steadfast and immovable in her love. She has persevered with joy through the long nights and trying days. This degree would not have been possible without you.

TABLE OF CONTENTS

ACKNOWLEDGEMENTS	iv
LIST OF TABLES	vii
LIST OF FIGURES	viii
LIST OF ABBREVIATIONS	ix
SUMMARY	xii
CHAPTER 1: INTRODUCTION	1
1.1 The Problem of Poor-Quality Medicines	1
1.2 Definitions	6
CHAPTER 2: CURRENT TECHNIQUES	9
2.1 Introduction to Current Portable Techniques for Detecting Poor-Quality Medicines	9
2.2 Chromatography	10
2.3 Spectroscopy	12
2.4 Colorimetry	15
2.5 Immunoassay	16
2.6 Microfluidics	16
2.7 Capillary Electrophoresis	17
2.8 Counterfeit Detection Device Version 3 Plus (CD3+)	17
2.9 Mass Spectrometry	18
2.10 Conclusions on Current Portable Techniques	20
CHAPTER 3: METHODOLOGY	22
3.1 Waters QDa Mass Spectrometer	22
3.1.1 Electrospray Ionization (ESI) Source	22
3.1.2 Ion Guides	26
3.1.3 Single Quadrupole Mass Analyzer	27
3.1.4 Photomultiplier Detector	33
3.2 Procedure	36
CHAPTER 4: RESULTS AND DISCUSSION	42
4.1 Total Ion Current (TIC) mode vs. Single Ion Recording (SIR) mode	42
4.2 Sample Results	44
4.3 Advantages	46
4.4 Disadvantages	48
4.5 Conclusions	50

APPENDIX: SUPPORTING INFORMATION
A.1: QDa Sample Data from all Active Pharmaceutical Ingredients (APIs) 52
A.2: Calibration Curves for Amoxicillin, Clavulanic Acid, Artemether,
Lumefantrine, Artesunate, Azithromycin, Dihydroartemisinin, Piperaquine . . . 56
REFERENCES 57

LIST OF TABLES

Table 1	Experimental parameters for all active pharmaceutical ingredients	38
Table 2	QDa sensitivity and specificity calculations	44
Table 3	QDa sample data for 7 active pharmaceutical ingredients	56

LIST OF FIGURES

Figure 1	Waters QDa mass spectrometer	23
Figure 2	Electrospray ionization (ESI)	24
Figure 3	Single quadrupole mass analyzer	28
Figure 4	Single quadrupole mass analyzer rods in the x-z plane	30
Figure 5	Bandpass mass filter created by single quadrupole mass analyzer	31
Figure 6	Photomultiplier detector	34
Figure 7	Photomultiplier tube (PMT)	35
Figure 8	Protocol for QDa experiments	39
Figure 9	Single ion recording (SIR) chromatogram for experimental run	41
Figure 10	Total ion current (TIC) mode vs. single ion recording (SIR) mode	43
Figure 11	Calibration curves of 4 active pharmaceutical ingredients	46
Figure 12	Calibration curves for 7 active pharmaceutical ingredients	56

LIST OF ABBREVIATIONS

A	Amoxicillin
AC	Alternating Current
ACT	Artemisinin Combination Therapy
AM	Artemether
API	Active Pharmaceutical Ingredient
ART	Artemether
AZITH	Azithromycin
CA	Clavulanic Acid
CD3+	Counterfeit Detection Device Version 3 Plus
CE	Capillary Electrophoresis
CEL	Cellulose
CI	Confidence Interval
CRM	Charged Residue Model
DART	Direct Analysis in Real Time
DC	Direct Current
DESI	Desorption Electrospray Ionization
DHA	Dihydroartemisinin
EDD	Erectile Dysfunction Drug
ESI	Electrospray Ionization
FCGQ	Field Collected Good Quality
GC-MS	Gas Chromatography Mass Spectrometry

GMP	Good Manufacturing Practices
GPHF	Global Pharma Health Fund
GSMS	Global Surveillance Monitoring System
HPLC	High Performance Liquid Chromatography
ICP-MS	Inductively Coupled Plasma Mass Spectrometry
IEM	Ion Evaporation Model
IMPACT	International Medicinal Products Anti-Counterfeiting Task-force
IMS	Ion Mobility Spectrometry
IMS-MS	Ion Mobility Spectrometry Mass Spectrometry
IP	Intellectual Property
IR	Infrared
LAC	Lactose
LED	Light-emitting Diodes
LC	Liquid Chromatography
LC-MS	Liquid Chromatography Mass Spectrometry
MRA	Medicine Regulatory Agency
MS	Mass Spectrometry
ND	Not Detected
OFLO	Ofloxacin
P	Piperaquine
PAD	Paper Analytical Device
PMT	Photomultiplier Tube
QDa	Waters QDa Mass Spectrometer

Q-TOF	Quadrupole Time of Flight
RF	Radio Frequency
RIT	Rectangular Ion Trap
RSD	Relative Standard Deviation
SIR	Single Ion Recording
SM	Sulfamethoxazole
STR	Starch
TB	Tuberculosis
TIC	Total Ion Current
TLC	Thin Layer Chromatography
TM	Trimethoprim
US FDA	United States Food and Drug Administration
USP	United States Pharmacopeia
WHO	World Health Organization

SUMMARY

Communities worldwide, especially in the developing world, are afflicted with poor-quality medicines disguised as genuine medicines used for treatment of common infections. Poor-quality medicines range from expired genuine tablets to placebos containing toxins created by criminals. Numerous patients are left with untreated conditions, financial losses, and little confidence in the health system. The developing world struggles to identify and quantitate poor-quality antimalarial and antibiotic medicines.

Portable devices employing robust laboratory techniques have the potential to turn the tide in this fight. Vast regions in the developing world lack laboratory analysis capabilities and therefore need portable instruments to perform medicinal quality evaluations. The portable devices lack the demonstrated capability to analyze all classes of poor-quality medicines. Results from tested devices reveal a significant gap in demonstrating the critical ability to distinguish poor-quality from genuine medicines.

This study evaluated the Waters QDa mass spectrometer in identifying and quantitating common antimalarial and antibiotic medicines. This instrument correctly identified all poor-quality medicines among 7 common pharmaceutical treatments. Using a high-throughput easily customizable method, the QDa characterized all poor-quality medicines, both falsified and substandard. This capability is unparalleled among portable instruments. The QDa possesses the ability to become an instrumental asset in the fight against poor-quality medicines.

CHAPTER 1

INTRODUCTION

1.1 The Problem of Poor-Quality Medicines

Poor-quality medicines posing as genuine, good-quality medicines deceive millions of unsuspecting victims every year leaving their conditions untreated causing financial loss, diminution of the public health system, and a multitude of preventable deaths. These poor-quality medicines include 3 types: falsified, substandard, and degraded [1-3]. Falsified medicines are fake medicines with labels containing false claims about the content and origin of the medicine. Substandard medicines are manufactured by authentic sources but fail to meet good quality standards. Degraded medicines are manufactured by authorized sources but have been spoiled through poor management along the supply chain rendering them outside of the good quality standards. Further definitions of these terms will be discussed in the section 1.2 [4-8].

The World Health Organization (WHO) established the Global Surveillance and Monitoring System (GSMS) to examine the pervasiveness of the poor-quality medicine issue including substandard and falsified drugs. In their first 4 years, antimalarials and antibiotics were by far the most reported poor-quality medicines accounting for 36.5% of the total reported medicines [9]. Poor-quality medicines infiltrate health systems all around the world the majority of which pervade regions hardest hit by infectious diseases, especially malaria [6, 9, 10].

Malaria has plagued mankind for centuries by infecting the red blood cells of the patient and is caused by the *Plasmodium* parasites and transmitted through female

Anopheles mosquitos [11]. Despite the advancements of modern medicine, malaria continues to claim scores of lives every year. In 2016, malaria cases climbed to an estimated 2.16 million worldwide; the largest total since 2012. The WHO estimates that 445,000 people died from malaria in 2016 [10]. The mortality rate decreased by 47% from 2000 to 2013 averting the deaths of an estimated 4.3 million people, but has gradually decreased by only 4.4% since 2013 [10, 12]. Other studies report even higher rates of morbidity and mortality [13]. With 3.2 billion people worldwide at risk for malaria and many cases and deaths left unreported, this disease has the potential to ravage populations for years to come [12, 13].

Antibiotics are also in high demand worldwide with the most pressing need in developing countries. These medicines treat common bacterial infections that range from inconvenient ailments to life-threatening illnesses [14]. Over nearly a century, antibiotics have improved the lives of people all over the world becoming a pillar of modern medicine [15]. It is estimated that over 1 million children perish each year from untreated cases of sepsis and pneumonia. Almost half of these deaths are children under the age of 5 in sub-Saharan Africa. Pneumonia was the second leading cause of death among children under the age of 5 in 2013 claiming nearly 935 million lives (preterm birth complications being the leading cause of death) [16]. The world needs good quality anti-infectives to treat malaria and bacterial infections, but unfortunately poor-quality medicines are a prevalent danger in the market.

Most of the literature quotes the WHO International Medicinal Products Anti-Counterfeiting Task-force (IMPACT) 2006 report finding that 10% of medicines worldwide are falsified [3, 11, 17-24]. The report goes on to state that in the developing

world defined as regions in Africa, Asia, and Latin America the falsified medicine estimates are safely between 10-30% [3, 17, 25]. When including all poor-quality medicines both falsified and substandards in the developing world the literature ranges from 10-50% of medicines [1, 11, 17, 19, 24-27]. Koczwara and Dressman (2017) assessed 54 studies covering the globe published between 2007 and 2016 verifying the often-cited claim that 10% of all medicines are falsified. The results vary widely depending on the region and method employed. They conclude that the available data do not support any definitive claims about the pervasiveness of falsified drugs or poor-quality medicines overall [26]. The literature contains other systematic reviews analyzing a multitude of studies investigating this issue revealing no definitive conclusions on the precise extent of poor-quality medicines. These studies varied greatly in sampling methods, techniques used for analysis, definitions (many had none), and packaging assessments among other parameters making them difficult to compare [11, 18-22, 24, 26, 27]. In many studies, it is uncertain to know if a random and representative collection of samples has been achieved [9] and difficult to secure legitimate genuine samples to verify results [28]. Comparing these studies illustrates the need for robust, systematic guidelines for future studies to produce quality data from strong methodology for any defensible conclusions to be produced [5]. Overall, the specific extent of poor-quality medicines is unknown.

Poor-quality medicines inflict grave consequences on the public health system, even opening an opportunity for drug resistance to spread. Resistance is a complex, multifaceted issue including many proposed mechanisms [29, 30] and theories of propagation [11, 31]. Although poor-quality medicines have not been proven to cause

resistance, modeling analyses indicate that inadequate dosing of patients opens a path for resistance to spread [11, 18, 30, 32, 33]. Substandard and some falsified medicines are contributing factors to inadequate dosing. The feasible pathway for spreading resistance comes about when a poor-quality medicine containing a sub-therapeutic amount of the active pharmaceutical ingredient (API) is used to treat a microorganism, it will not be eradicated, but instead adapt allowing it to survive despite the presence of drugs and transmit the resistance through other hosts [11, 31, 32]. Drug-resistant mutations contribute to treatment failure in which the medicine is unable to eliminate the microorganism or resolve the symptoms [11, 31]. In 2016, the WHO reported that 490,000 individuals developed tuberculosis (TB) that was multi-drug resistant noting that drug resistance is major issue with malaria as well [34]. Antimalarial resistance by parasites could render current treatments futile and fuel a rise in the mortality rate worldwide [12].

Falsified medicines can contain toxic levels of impurities and/or incorrect APIs causing harmful effects on patients even causing death. Other falsified medicines contain correct levels of APIs treating the condition yet robbing the genuine medicine manufacturer of profit and possibly containing impurities [26]. Samples of poor-quality medicines were found to contain substandard levels of APIs prolonging the illness, while others contained toxic levels of APIs causing harm to the patient [20]. In addition to the harmful physical effects of poor-quality medicines, the economic impact extends throughout the healthcare system. Patients lose hard-earned money on medicines that fail to deliver. Legitimate medicine manufacturers suffer both financial and reputational losses due to criminal production of poor-quality medicines [14, 26]. A cost analysis

study extrapolated a scenario projecting a 10.5% poor-quality medicine rate applied to a low or middle income market size, then a loss of around US\$ 30 billion would be endured in that market [9]. With other estimates reporting higher rates of poor-quality medicines, the financial loss felt around the world is crippling. The major issues caused by poor-quality medicines including drug resistance, adverse even deadly health effects, ineffective treatment, financial loss among others have created a loss of confidence in the health system especially in the developing world [1, 3, 9, 18, 26, 31].

Globalization advances healthcare around the world, yet also enables criminals to manufacture, distribute, and trade poor-quality medicines. The technology and expertise available for all to acquire produces avenues for delinquents to infiltrate the public health system [2, 3, 9, 23, 26, 35]. Organized crime has laid hold of this opportunity that has become a lucrative business with high profit margins [9, 20, 22]. The pharmaceutical industry is riddled with entry points for criminals to inject their supply of falsified medicines from manufacturing through wholesalers and pharmacies creating an extensive and complex problem [9, 12, 22]. One of the most discouraging contributing factors is the insufficient legislation and enforcement from governments, especially in the developing world. Current laws are woefully incapable of addressing the problem, especially as the medicines permeate international trade, and enforcement is crippled by corruption and lack of resources [9, 14, 18, 22, 23, 26]. In the developing world, medicinal quality assurance is lacking. Current systems are incapacitated by the lack of resources, screening technologies, and expertise throughout the supply chain to assess the quality of medicines [9, 10, 22, 36]. The immense issues involving poor-quality medicines have far-reaching, devastating effects mostly inflicting the developing world.

1.2 Definitions

Genuine or good quality medicines are generally defined as products created by legitimate, authorized manufacturers following Good Manufacturing Practices (GMP) that pass the quality assurance specifications as laid out by the Medicine Regulatory Agency (MRA) and continue to follow those standards throughout the entire process including the full-term treatment of the patient. Legitimate medicines must be produced by traceable, sanctioned manufacturers and maintain quality in order to perform their intended function with no unforeseen side-effects [9, 24, 26]. The specifics of definitions are of major importance in identifying and addressing poor-quality medicines.

Universal definitions characterizing specific classes of poor-quality medicines are critical but have long been disagreed upon. Since no global set of definitions govern the used of these terms confusion and misinterpretation have ensued. Common definitions would harmonize future studies revealing the true extent of poor-quality medicines [11, 22, 26]. The WHO established definitions used by most for classification starting in 1992 [7] undergoing various revisions to deal with complications and nuances [4, 37]. Generally, the latest WHO definitions have been used to scope the types of poor-quality medicines [1-3, 5, 24, 26, 35]. Most recently, the WHO clarified the recent set of definitions [38] in 2017 adapting the working definitions which serve as the basis used in this thesis [8].

Substandard medicines are also known as “*out of specification*” defined as “*authorized medical products that fail to meet either their quality standards or their specifications or both.*” [8]. These include medicines produced by an authorized manufacturer that fail to pass the quality requirements as dictated by the MRA [2, 4, 6].

A key factor involving substandard is that the authorized manufacturer had no nefarious motives but rather failed to follow GMP [3].

Degraded medicines are also produced by registered manufacturers following GMPs passing the MRA criteria but later deteriorate outside of the quality standards. This is commonly due to a failure to transport or store the medicine under proper conditions along the supply chain allowing for the degradation of the components [4, 24]. Exposure to harsh climates or direct sunlight can accelerate the degradation of a medicine. The use of ‘degraded’ is not as prevalent in the literature as the other two terms since many MRAs lack the ability to distinguish degraded from substandard medicines. The distinction between degraded and other poor-quality medicines especially substandard are critical to correcting the issue [24, 26].

Falsified is the term typically used when discussing public health considerations and are defined as *“medical products that deliberately/fraudulently misrepresent their identity, composition, or source. Any consideration of intellectual property rights does not fall within this definition. Such deliberate/fraudulent misrepresentation refers to any substitution, adulteration, reproduction of an authorized medical product or the manufacture of a medical product that is not an authorized product.”* [8]. The key aspect of falsified medicines is the intentional falsification of a product with regards to the packaging, information, components, manufacturer, or any point along the supply chain. Falsified medicines could contain the correct API(s) and even within the MRA standards but are misrepresenting a different aspect of the medicine. The WHO recognized the term “counterfeit” brought on Intellectual Property (IP) rights concerns from pharmaceutical companies clarifying the term “falsified” to focus on public health concerns. This issue

has caused debates between the two pressing issues of focusing on the health of patients but also providing for the prosecution of criminals [4, 24, 26].

In general, the poor-quality medicines referred to in the literature fall under either substandard, falsified, or degraded with counterfeit used when legal ramifications are discussed. Adopting universal definitions is paramount in the fight against poor-quality medicines framing studies, influencing legislation, and enabling the scientific community to address the pressing issue using the same terminology.

CHAPTER 2

CURRENT PORTABLE TECHNIQUES

2.1 Introduction to Current Portable Techniques for Detecting Poor-Quality Medicines

This chapter will serve as an abbreviated overview of the current portable techniques highlighting relevant specific devices used for identification and quantitation of poor-quality medicines. The term ‘portable’ refers to equipment intended to be fully functional when deployed into the field, able to be moved by one or two people, with minimal set-up required. This does include techniques requiring initial start-up by an experienced technician such as the construction of a reference library [39, 40]. After initial set-up, the portable technique will be trainable and straightforward for technician-level operators. Numerous studies failed to include key details such as the sensitivity and specificity of the device along with the APIs assessed and a low sample size limiting their usefulness [41-44]. The term ‘sensitivity’ refers to the ratio of medicines determined to be poor-quality by the device compared to the total number of poor-quality medicines as identified by the reference technique. The term ‘specificity’ refers to the ratio of medicines determined to be authentic by the device compared to the total number of genuine medicines as identified by the reference technique. The challenge with portable instruments is miniaturizing complex techniques into robust, trainable and well-tested devices demonstrating the capability to identify and quantitate poor-quality medicines. A wide range of techniques are represented by portable devices with various levels of complexity, nuance and proven ability to handle various types of poor-quality medicines.

2.2 Chromatography

High Performance Liquid Chromatography (HPLC) is often used for laboratory confirmation testing of poor-quality medicines as the reference technique [26, 41-46]. This technique uses a column containing a stationary phase through which the sample mixture and mobile phase are forced through separating out the components of the sample mixture by their affinity to the stationary or mobile phases. The identity and quantitation of the components can be determined by comparing the retention times and peak integrations to authentic products [42, 44]. In the developing world, the MRAs lack the time, finances, and availability to perform confirmatory analysis from a formal laboratory. Frequently the process from collection of suspect medicines through reception of test results gives enough time for the poor-quality medicines to permeate the market [42-45]. Although HPLC and LC in general is a highly sensitive technique currently it still requires facilities, resources, and highly-technical training preventing it from deploying into the field [45]. Recently, a study presented the potential for a miniaturized, portable LC device capable of in-field analysis [40]. The C-Vue [47], a portable laboratory liquid chromatograph, is an inexpensive table-top unit able to separate and detect analytes exhibiting UV absorbance. This device demonstrated a specificity of 60% and a sensitivity of 100% for both falsified and substandard medicines when tested using 5 APIs [40]. The C-Vue is limited to APIs displaying UV absorbance, limiting the number of potential analytes. Also, a fair amount of sample preparation and data analysis training is needed, but the sensitivities of this device especially for determining substandard medicines across 5 APIs is unmatched in the literature creating a case for

further testing and in-field analysis. Apart from this study, no other portable liquid chromatography devices have been reported.

The most widely used in-field device is the Global Pharma Health Fund (GPHF) Minilab employed in 97 countries, many in the developing world [48]. Over 800 Minilab cases have been sold worldwide. This device implements a 3-part method including a physical inspection for dosage and packing, a dissolution test, and thin-layer chromatography (TLC). In TLC, a small drop of diluted sample is placed on the silica plate used as the stationary phase. The bottom of the silica plate is then dipped into a mobile phase. Capillary action soaks up the mobile phase which interacts with the sample separating out the constituents. The distance traveled and darkness of each spot determine the identity and relative concentration of the sample [42, 44, 46]. The semi-quantitative Minilab or “lab-in-a-suitcase” contains benchmark TLC standards made at 50%, 80%, and 100% of the API for comparison with a sample [46]. The Minilab succeeded in identifying the presence or absence of an API, but the variability between analyst interpretation of the results leaves this technique only semi-quantitative [26, 44, 46, 49, 50]. In a WHO study performed across 6 countries in Sub-Saharan Africa only 32% of the poor-quality medicines were identified by the Minilab [51]. In Tanzania, 4 different APIs (antimalarials and antibiotics) dispersed among 28 samples at 3 concentrations of 0%, 40%, and 100% of the API analyzed using the TLC method in the Minilab. In the first analysis 25 of the 28 substandard samples with 40% API were inaccurately identified as being genuine quality. Upon further training, 8 of the 28 were again inaccurately identified as being genuine quality [51]. Also in Tanzania, a proficiency test led by the country’s Food and Drugs Authority revealed only 5 out of 9 veteran analysts

correctly characterized antimicrobial API levels using this method [52]. On the other hand, in Ghana a field survey was conducted containing 14 poor-quality medicines amongst 84 antimalarials. The TLC results demonstrated 100% specificity and sensitivity compared to the reference technique [53]. One study tested 506 samples including 5 common antimicrobials for evaluating the Minilab against HPLC. The frequency of poor-quality medicines as determined by the Minilab compared to HPLC, respectively, was 0% versus 14.9% for amoxicillin and 0% versus 17.4% for azithromycin [49]. Overall, 77 samples determined to be good quality by the Minilab were in fact poor-quality medicines generating a false-negative detection rate of 15.2% [49]. Many of these samples contained between 80-100% API concentrations for which the Minilab is not designed to detect [46, 49]. While some studies reveal success, overall the Minilab demonstrated unsatisfying results in identifying poor-quality medicines, especially substandard medicines with API levels close to genuine, further illustrating the variability of this technique [26, 44, 46, 49]. The manuals developed for the Minilab were employed in this study for the extraction portion of the sample preparation.

2.3 Spectroscopy

Spectroscopic techniques are the most widely used among portable devices for quality drug control. These techniques irradiate the sample with specific wavelengths of light instigating molecular vibrations or electronic excitation causing the sample to emit or absorb the electromagnetic radiation. The light emitted or absorbed is collected as spectra. The spectra produced, called a 'fingerprint', is specific to the chemical composition of the sample and is compared to a reference library of spectra for a match

[43, 44, 54]. These widely available techniques are easy to use, require little or no sample preparation involving no reagents, and are noninvasive and nondestructive to the sample. [42, 43, 45, 55-57]. Also, some of these handheld spectrometers allow for in-package analysis of medicines yielding further information for quality assessment [44, 54, 57].

Infrared (IR) spectroscopy is commonly employed in handheld devices utilized in pharmaceutical analysis, but very few show potential for quantitative analysis of poor-quality medicines [40, 43, 44, 55, 56, 58]. In IR spectroscopy, the sample is irradiated using IR radiation with the transmitted light measured as a spectrum. Certain chemical bonds will absorb radiation at characteristic wavelengths and intensities creating a distinctive spectrum used to identify the molecule [55, 56, 58]. The MicroPhazir, studied by Guillemain et al. (2017), presented a sensitivity and specificity of 100% in discriminating genuine and falsified samples with substandard samples absent from this study. A key parameter for this instrument, the correlation distance limit, varied depending on the medicine type and established through experimentation with genuine medicines [56]. This deepens the complexity of the technique potentially causing issues in future in-field use along with the complex mathematical models employed [56]. In the same study, the SCiO manufactured by Consumer Physics displayed the same level of results for falsified medicines. The smartphone-sized SCiO employed in a separate study detected falsified medicines with 100% sensitivity along with quantitation of artesunate concentrations within $\pm 14.8\%$ with 95% certainty among 15 samples [56]. Unfortunately, quantitation was not achievable for the other single API, amodiaquine, and none of the combined APIs tested in the study [55].

Raman spectroscopy is another common technique employed within portable devices [40, 42-44, 50, 54-57, 59]. In Raman spectroscopy, a sample is irradiated with electromagnetic radiation most of which is transmitted through the sample while a small portion is scattered in all directions. Rayleigh scattering, the majority of the scattered light, is elastic since the scattered light frequency is identical to the incident radiation, meaning the electron began and ended in the same vibrational state [54, 59]. Raman scattering is inelastic since the scattered light frequencies are lower (Stokes scattering) or higher (anti-Stokes scattering) compared to the incident radiation. Raman spectroscopy measures the inelastically scattered radiation emitted by the sample producing a characteristic spectrum revealing the structure of the molecule [54, 59]. The TruScan Raman spectrometer, one of only six field tested devices [39, 44, 53], identified falsified medicines with a sensitivity of 100% and a 99% specificity [53]. The study also evaluated products comprised of a 50% or 150% API content. The device determined all 4 samples passed revealing the difficulty in characterizing substandards with this device [53]. A study by Hajjou et al. (2013) also illustrates the issues with TruScan deciphering differences in API strengths between genuine and substandard medicine yet specificity and sensitivity calculations were absent. Another handheld Raman device is the NanoRam manufactured by B&W Tek [60]. An investigation testing 289 antimalarial samples using the NanoRam displayed a 100% sensitivity and 96% specificity when determining falsified medicines. Substandard medicines were neglected but identified as a potential issue for this device [60]. Raman spectroscopy is limited to analytes not displaying fluorescence which saturates the detector making a fingerprint impossible to decipher. Fluorescence plagues Raman spectroscopy by exciting many sample

components masking the informative scattering signals [39, 59]. Additionally, questions remain over combination medicines with one API producing a strong Raman scattering signal possibly overwhelming the Raman scattering created by another API [39]. This technique also had issues with generic and placebo medicines not performing as expected [54, 57, 59].

Spectroscopic techniques have some challenges in assessing poor-quality medicines. For any spectroscopic technique, the irradiating energy must be resonant with the analytes to a detectable level. Handheld devices typically display higher noise and lower signal intensities when compared to laboratory instrumentation making some medicinal products more difficult to analyze especially low-dosage products [45, 54, 57, 61]. A reference library is needed for these techniques containing comparison spectra that vary depending on API and excipient content as well as brand requiring consistent updating and compilation of genuine samples from pharmaceutical companies which has proven to be difficult [44, 60]. Also, the coating of certain medicines will likely cause issues in analysis using spectroscopic techniques [54, 59]. Overall, spectroscopic techniques have demonstrated success in packaging assessment, physical analysis, and formulation screening of medicines with some devices able to decipher between genuine and falsified medicines yet in general demonstrate significant difficulty distinguishing between genuine and substandard medicines [40, 42-45, 53, 54, 56, 57, 59].

2.4 Colorimetry

One device best demonstrating a colorimetric technique is the Paper Analytical Device (PAD) [62, 63]. The PAD developed to aid in-field medicinal screening as a low

cost, easy to use technique has presented promise with identifying falsified medicines. This single-use paper card contains 12 colorimetric chemical tests each giving information about the contents of the medicine with limitations on the types of APIs available for testing [62]. Prolonged exposure to hot, humid conditions common throughout the developing world will deteriorate the capabilities of the PAD the full extent of which is unknown [62]. PADs have been tailored to analyze certain pharmaceutical medicines such as the antibiotic PAD (aPAD). An investigation using the aPAD for quantitative analysis found that 11 out of 50 (22%) amoxicillin substandard samples and 7 out of 28 (25%) ampicillin substandard samples were incorrectly determined to be genuine. Multiple samples contained API levels between 85-89% while the rest of the samples were thermally stressed in the lab possibly influencing the results [63]. Colorimetric techniques demonstrated success in identifying the APIs yet require sample preparation and display unsatisfying results when analyzing substandard medicines.

2.5 Immunoassay

Artemisinin-based combination therapies (ACT) were assessed using immunoassay dipsticks specific to each type of ACT. Medicine samples are extracted and diluted with a few drops distributed onto the dipstick. Color indicators on the dipstick reveal the API contents, similar to a pregnancy test [64]. The dipsticks are one of the few field-tested techniques analyzing samples from Colombia, India, Papua New Guinea, and Zambia. The results of the ACT study did not publish specificity or sensitivity calculations, but they were able to identify the correct APIs in the samples [64].

Immunoassay techniques have the potential for further in-field implementation with the benefits of no power requirements, low cost, transportable worldwide, and ease of use. One major drawback is the antibodies must react with the specific API being assessed, meaning each device will be specific to an API potentially causing confusion with operators [64]. This device identified the presence of targeted APIs, yet only displayed semi-quantitative capabilities and assessed one medicine type. Further testing is needed to determine the stability of the dipsticks in tropical climates over time, the tailoring of dipsticks to other APIs, and their ability to perform quantitative analysis [44, 64].

2.6 Microfluidics

The best example of a fieldable technique based on microfluidics is the PharmaChk device. This is an in-field, prototype device performing a dissolution test along with attaching luminescent reagents specific to the API to measure results using luminescence [40, 44, 65]. The developers at Boston University continuously incorporate user feedback from operators in Ghana to make the device easier to use. The results are promising with 0-4% difference compared to the reference technique of HPLC [65]. In the future, the goal of this device is to employ a design capable of analyzing multiple APIs without necessitating a reference library but currently this device has only tested artemisinin-based drugs [40, 65]. This device requires detailed standards preparation and uncommon reagents that degrade only hours after preparation [40, 65]. Further testing using other APIs needs to be completed before widespread use will be achieved.

2.7 Capillary Electrophoresis

Capillary electrophoresis (CE) is a technique separating charged analytes based on their movement through a small channel directed by a high electrical field. The benefits include no stationary phase, short experimental run time, high separation efficiency, and low maintenance. When miniaturized this has shown potential to address the problem of poor-quality medicines yet the sample size, sensitivity, and specificity were absent [66]. While the instruments are low cost, robust, and portable, they continue to involve more reagents in complicated mixtures requiring precise pH values, convoluted set-ups and data analyses increasing the complexity of the technique [66-68]. More pharmaceutical testing is needed using additional antimalarial and antibiotic medicines, large sample sizes, specificity and sensitivity calculations and while deployed in the field.

2.8 Counterfeit Detection Device Version 3 Plus (CD3+)

The United States Food and Drug Administration (US FDA) developed a low cost, battery powered device to analyze the packaging and contents of suspected poor-quality medicines called the Counterfeit Detection Device Version 3 (CD3+) and has been deployed to Ghana [42, 45, 53, 69, 70]. This device equipped with several light-emitting diodes (LEDs) each shining a single wavelength to monitor the sample response while using cameras to capture the images. These images can be compared with the built-in library or a genuine sample if attainable [69]. This device demonstrated a 100% specificity and 98.4% sensitivity when determining counterfeit artesunate samples in one

study [69]. Another investigation involving 84 samples compared the CD3+ against the Minilab and TruScan devices with HPLC confirming the results. The CD3+ only had a specificity of 64% but a 100% sensitivity when weeding out falsified and substandard drugs. The study failed to distinguish the specific sensitivities for falsified and substandard medicines [53]. This device showed difficulty in identifying genuine samples due to variations in packaging from authentic manufacturers. The CD3+ enables straightforward, rapid analysis and is substantially less expensive compared to other techniques [53]. Further testing is needed evaluating separate categories within poor-quality medicines including falsified and substandard medicines.

2.9 Mass Spectrometry and Ion Mobility Spectrometry

Throughout the world, the need is great for in situ chemical analysis to not only identify but also quantitate APIs to aid the fight against poor-quality medicines. Mass spectrometry (MS) is a powerful technique with potential to address this issue especially as more miniaturized instruments emerge. This technique contains three steps: ionization of the analyte(s), sorting and selecting of ions, and detection of the ion abundances with a specific mass to charge ratio. The mass to charge ratio corresponds to the potential identity of the ion based on molecular formula. Quantitative analysis correlates the observed ion abundance with the concentration of the analyte. This technique involves sample preparation typically using common reagents and specific standards to compare against sample results [44, 71-73]. While the initial cost and training for MS exceeds others [44], the capability to quantitate APIs surpasses that of the spectroscopic techniques described above.

Ion mobility spectrometry (IMS) proven to be a high-throughput and sensitive technique requiring little sample preparation has been implemented into rapid screening devices [71-73]. IMS separates ions based upon their ion mobility in the gas phase using their drift time across a tube filled with an inert drift gas and guided by an electric field for identification. The movement of gas phase ions depends upon the charge, shape, and size of the ions [71, 72]. This rapid, highly sensitive technique achieves low detection limits and does not require solvents, although a buffer gas is required [72]. The SABRE 4000, manufactured by CBRN Tech Index, employed in an investigation of dietary supplements to analyze sibutramine in low abundance demonstrated the ability to analyze samples with a concentration as low as 2 ng/ μ L [71]. The IONSCAN-LS portable IMS-MS operating in positive mode showed potential in a study detecting synthetic erectile dysfunction drugs (EDD) along with their analogues. The device detected all of the APIs, synthetic and analogues, in all 26 herbal supplements tested proving a 100% sensitivity and specificity yet was unable to successfully discriminate the identity of two contaminants due to their similar mobilities [72].

The Mini10 handheld mass spectrometer coupled both Desorption Electrospray Ionization (DESI) and Electrospray Ionization (ESI) methods with a rectilinear ion trap (RIT). While using ESI, this device detected drugs of abuse to the parts-per-billion range in an aqueous mixture, but currently there is no assessment of this device in identifying poor-quality medicines [74].

The Waters QDa mass spectrometer used in this study was previously coupled to Direct Analysis in Real Time (DART) ambient ionization to provide rapid chemical fingerprinting of antimalarials coupled to a low cost, portable mass spectrometer. This

set-up accurately characterized specific compounds in 192 falsified antimalarials. When spectra were compared to a high-resolution quadrupole time of flight (Q-TOF) it revealed the loss of very low abundance species, but the base peaks matched in both spectra displaying corresponding fingerprints [75]. Only one type of antimalarials were tested, the artemether and lumefantrine based ACT, and the ability to quantitate was not assessed but left as a potential for future investigation [44, 75]. This thesis will detail the assessment of the QDa to identify and quantitate the stated APIs in antimalarial and antibiotic medicines using an electrospray ionization ESI source.

2.10 Conclusions on Current Portable Techniques

Despite the range of current portable techniques, a great need remains for highly sensitive in-field devices to detect and assess all types of poor-quality medicines. A thorough review of the literature revealed over 5,718 reports evaluated for portable, in-field analysis potential narrowing the scope down to 41 portable devices to be assessed [44]. After a detailed evaluation of these devices, the authors found a significant lack in sensitivity data vital for protecting patient health and the median sample size for each device was a meager 2 (1-20) or the tested APIs were not stated at all. Several devices demonstrated strong prospective for qualitative analysis, but few were evaluated for discovering substandard medicines with even less demonstrating the capability to distinguish them from genuine medicines [44]. The training time, implementation cost, maintenance, and cost-effectiveness of investing in each device has not been thoroughly analyzed [44]. Highly sensitive techniques are often more expensive and difficult to develop into a portable version, while many current portable devices are semi-

quantitative at best and usually require highly experienced technicians using complicated methods for each individual API [42-45]. Therefore, it is a necessity to develop, thoroughly test, and implement devices capable of in-field qualitative and quantitative analysis to address the immense problem of poor-quality medicines [9, 36, 44, 75].

CHAPTER 3

METHODOLOGY

3.1 Waters QDa Mass Spectrometer

In support of the ongoing instrument evaluation effort [40, 44] this study evaluates the Waters QDa mass spectrometer (QDa) for rapid analysis of poor-quality medicines [76]. This mass spectrometer is designed to be streamlined and straightforward from set-up through data analysis yielding mass spectral data with less complexity than typical mass spectrometric methods [76-81]. The term mass detector used to describe this instrument emphasizes the simplicity and user-friendliness of this instrument by limiting ionization parameters and API specific settings alteration needs along with eliminating manual calibrations [79, 81]. The QDa has been utilized in drug discovery [79], identification and quantitation of drugs of abuse [80], quality control [77], and quantitative analysis [78, 81] often coupled with chromatographic separations [77-81].

Mass spectrometers have three main units including the ionization source, mass analyzer, and detector. For this study, the QDa employed an electrospray ionization (ESI) source, a series of ion guides, a single quadrupole mass analyzer, and a photomultiplier detector (Figure 1). Section 3.1 will briefly explain these specific units.

3.1.1 Electrospray Ionization (ESI) Source

The ESI source disperses a solution into an aerosol spray transferring analytes from the liquid to the gas phase using an electric field priming ions for analysis using mass spectrometry [82-87]. In the 1960s, Malcom Dole, observed mechanics painting

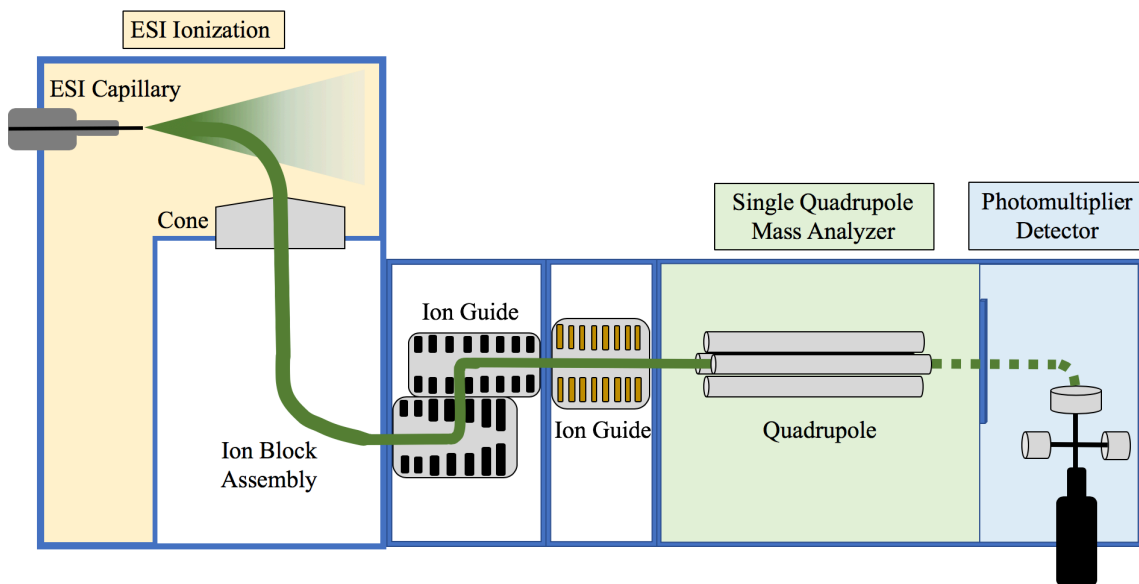


Figure 1: Schematic of the Waters Qda mass spectrometer set-up (not to scale).

cars using electrospray creating tiny charged droplets applying the paint evenly across the surface. Inspired by the mechanics, Dole coupled the ESI technique with a mass spectrometer [83-85, 88]. This soft ionization technique solved the issue of analyzing macromolecules using mass spectrometry in a rapid and efficient manner with minimal fragmentation [83-85]. Over time, ESI has been a choice technique in analyzing biomolecules [83, 85, 89-91], paired with a variety of separation techniques especially LC [85, 92, 93], and used in API analysis [94-97]. This robust ionization source has been proven to effectively ionize molecules of various sizes, shapes and charges [83, 84, 90, 98]. ESI is capable of generating either positive (positive mode) or negative ions (negative mode). This study used positive mode for most APIs therefore the following mechanism description will assume positive mode analysis. Negative mode analysis follows the same mechanism except all charges are the opposite of positive mode. ESI has three major stages including the formation of charged droplets, reduction of charged

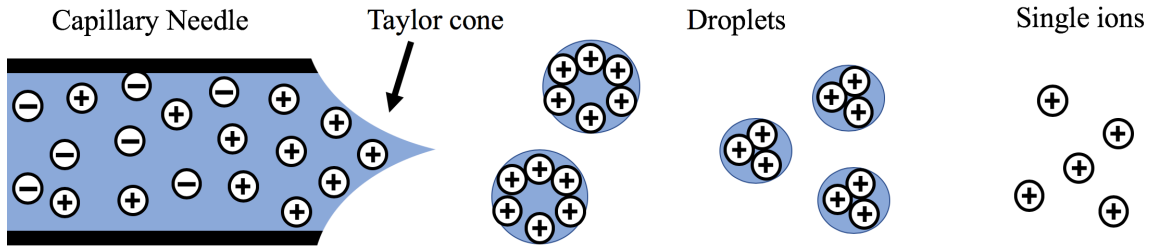


Figure 2: Schematic of electro spray ionization (ESI) with the Taylor cone forming at the tip of the capillary needle releasing droplets that subsequently evaporate liberating single analyte ions.

droplet size, and liberation of gas phase ions from the droplets (Figure 2) [82-87].

Through these stages, ESI transfers analytes from solution to gas phase ions.

The protic or aprotic solution used to introduce the analyte into the ESI source contains water, methanol or a combination thereof often with small amounts of a weak acid or base in order to ensure complete solubility and ionization of the analyte [83, 84, 87].

In the initial step, ESI creates charged droplets from the incoming solution (Figure 2). First, the solution containing the analyte is pumped through a capillary inside the probe into the first compartment held at atmospheric pressure. A high voltage is applied to the capillary creating an electric field permeating through the solution [82, 84]. The electric field induces charge separation migrating the positive ions toward the tip of the capillary [83, 85]. The buildup of positively charged ions destabilizes the meniscus causing a particularly shaped cone to form called the Taylor cone (Figure 2) [82, 84, 99, 100]. Inside the Taylor cone, the positive ions accumulating near the end of the cone cause an increase in the Coulombic repulsion of the surface charge. Eventually, this repulsion is equal to the surface tension of the solution, a point termed the Rayleigh limit

[82, 83, 85, 100, 101]. When the repulsion surpasses the Rayleigh limit, a jet of fine droplets is sprayed from the Taylor cone into the open air. Each droplet contains an excess of positive ions coming off the tip due to the amassing of positive ions [84, 86].

As these charged droplets drift away from the Taylor cone, the positive ions accumulate around the surface of the droplet. The solvent within the droplets evaporates aided by the heated capillary and the desolvation gas, nitrogen in the case of the QDa [79, 83, 84]. As the solvent evaporates the droplets decrease in size bringing the positive ions closer together thus increasing the repulsion force until it overcomes the surface tension expelling a stream of progeny droplets in a process called Coulomb fission [82, 85]. Experiments completed by Gomez and Tang (1994) captured images depicting a stream of progeny droplets emitted from a parent droplet, creating an almost miniature Taylor cone [102]. This process of evaporation and fission of the droplets from parent to progeny droplets leads to tiny charged droplets becoming the precursors to the gas phase ions (Figure 2).

The final stage of ESI entails the liberation of gas phase ions from the tiny charged droplets (Figure 2). The mechanism by which this final stage progresses is described by two prevailing theories. The first method is the charged residue model (CRM) first proposed by Dole analyzing molecules with high molecular weight [83, 84, 88]. This model predicts that the continuous evaporation of the solvent around the charged analyte leads to many droplets with a single analyte ion inside. The analyte is liberated into the gas phase by evaporation of the remaining solvent [82-85, 103]. This theory is typically used to explain the mechanism by which large macromolecule ions reach the gas phase [83, 84, 103].

The ion evaporation model (IEM) developed by Iribarne and Thomson (1976) describes their work with small ionic analytes including sodium and chloride ions [104]. Based on their experimental results [104] and theoretical calculations [105] Iribarne and Thomson theorize that ions collect around the surface of the droplets and directly emit from the surface once the droplets decrease to a radius of less than 10 nm [83, 84]. Their results led them to conclude that larger molecules followed the CRM process while the smaller ions proceeded by the IEM [84, 104, 105]. In IEM, when the droplets become sufficiently small, less than a 10 nm radius, ion evaporation replaces Coulomb fission expelling the charged ions accumulated on the outer surface of the droplets [83, 84, 104, 105]. In this final stage of ESI, ions are liberated from the small droplets by either the CRM or IEM ready to proceed on to the mass analyzer.

3.1.2 Ion Guides

The successive combination of chambers containing ion guides (Figure 1) uses electric field and pressure gradients to focus the stream of positive ions into the mass analyzer while filtering out neutral, and negative ions. After ESI sprays all species, neutral and ionic, into the air, the positive ions must be selected for analysis. Nitrogen gas is channeled along the capillary following the trajectory of solvent drying out the droplets as well as driving the neutral species away from the opening to the mass spectrometer, the cone (Figure 1) [82-85]. Along with the nitrogen, the capillary is heated to assist in the evaporation of the droplets [84]. The positive ions produced through ESI are electrostatically attracted to the cone by the voltage applied. This cone, orthogonal to the capillary, guards the entrance to the second chamber containing a lower pressure than the

ambient pressure in the first chamber funneling the ions into the ion guides (Figure 1) [82, 85]. The sequence of chambers throughout the mass spectrometer each have lower pressure than the previous chamber, creating a pressure gradient attracting the flow of ions through the ion guides and mass analyzer to the detector [79, 83, 85]. The off-axis ion guides use electrostatic forces to guide positive ions around successive bends while sifting neutral ions out of the stream. The next ion guide contains conjoined, stacked rings forming the optimal stream of positive ions primed for the mass analyzer [82-85]. The use of ion guides assists in eliminating neutral noise along with improving the limit of detection and robustness of the instrument [79, 82, 84]. The nitrogen gas along with the heated capillary aid the rapid formation of gas phase ions while the electric field and pressure gradients create a highly efficient ion transmission through the ion guides focusing the optimal stream of ions prepared for the single quadrupole mass analyzer [82-85].

3.1.3 Single Quadrupole Mass Analyzer

Single quadrupole mass analyzers are utilized across the field of MS including gas chromatography MS (GC-MS) [106-108], LC-MS [109-111], and inductively coupled plasma source MS (ICP-MS) [112-114]. Multiple quadrupole mass analyzers can be arranged in succession gaining further information increasing the analysis capability in a method termed tandem MS-MS [115-119]. The single quadrupole mass analyzer mimics the properties of a runnable bandpass mass filter allowing only a narrow band of molecules of a particular mass to charge ratio (m/z) to pass through traversing ahead toward the detector [120, 121]. This single quadrupole is referred to as a mass filter

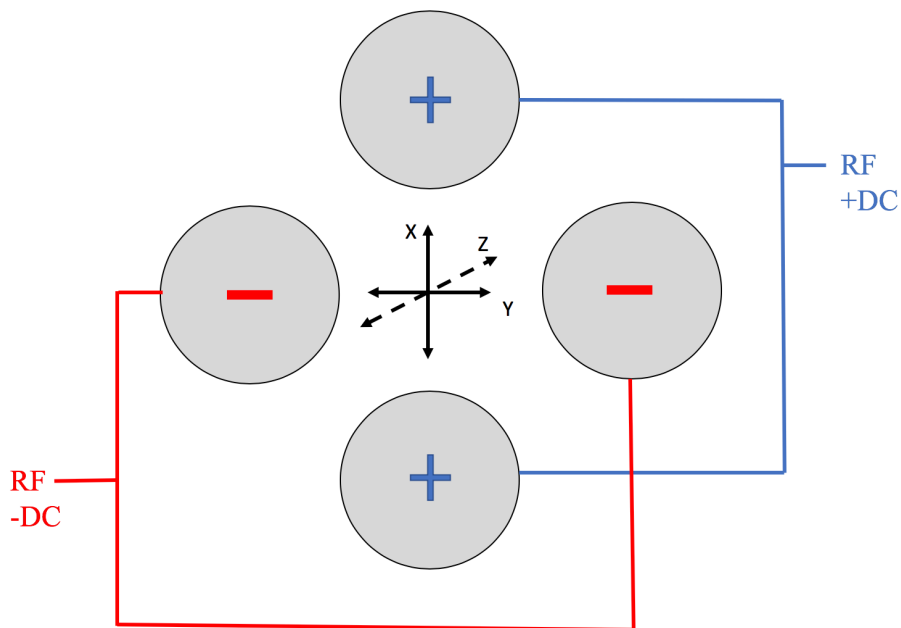


Figure 3: Single Quadrupole Mass Analyzer configuration showing the two pairs of rods acting as electrodes. One pair has the +DC voltage and oscillating RF voltage (blue) while the other pair has the -DC voltage and oscillating RF voltage (red). From this vantage point the x-axis is vertical, the y-axis is horizontal, and the z-axis is going into the page.

because of this aspect. The mechanical simplicity allows the creation of a compact mass analyzer to achieve high ion transmission. In addition, the low cost, light weight, high scan speed, robustness, easily tunable scanning modes, and low power requirements make this mass analyzer uniquely advantageous for portable devices [81, 120-122]. Portable devices employing this mass analyzer achieve sensitive, high throughput capability typically exhibiting unit mass resolution [81, 122].

The single quadrupole is made of four identical cylindrical rods acting as electrodes arranged in parallel along the central axis, z axis (Figure 3). Another option is to integrate hyperbolic rods rather than cylindrical, although the QDa contains cylindrical [78, 79, 86]. The rods opposite each other are linked electronically with one pair linked to

the positive terminal of the direct current (dc) voltage source and the other pair linked to the negative terminal. A variable alternating current (ac) is applied to each set of rods as well [86, 87, 121]. These ac currents are 180° out of phase with a frequency in the radio frequency (RF) range and alternate between positive and negative voltages with each pair of rods opposite in sign but equal in magnitude [120, 121]. The combination of the dc and ac voltages applied to the four rods creates a mass filtering operation allowing molecules with a specific mass to charge ratio to hold a stable trajectory completing successful passage on to the detector. One pair of rods is in the x-z plane with a positive dc voltage while the other pair of rods is in the y-z plane charged with a negative dc voltage of the same magnitude (Figure 3) [123, 124]. In order for an ion to transmit through the mass analyzer and reach the detector it must navigate a stable trajectory in both the x-z and y-z planes [86, 87].

The pair of rods in the x-z plane are charged with a positive dc voltage and an alternating RF voltage. When only the alternating ac voltage is applied to a beam of incoming ions, the alternating sign attracts and repels the ions toward and away from this pair of rods (Figure 4) [86, 120, 121, 125]. While the rods are charged with a positive potential, the positive traveling ions are pushed away from the rods towards the z or center axis. During the other half of the cycle when the rods are charged with a negative potential the positive ions are attracted towards the rods away from the center axis [87, 123]. While the negative voltage is applied and an ion hits a rod, it is neutralized and eliminated from the beam of ions. Whether or not a positive ion strikes a rod depends on multiple factors including the rate of movement along the z axis, mass to charge ratio of the ion, and magnitude and frequency of the ac voltage [120, 121]. When the positive dc

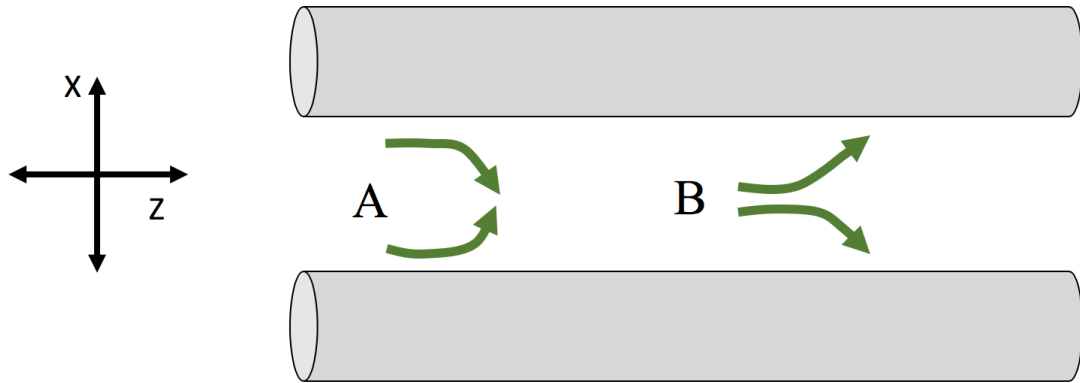


Figure 4: Single quadrupole mass analyzer rods in x-z plane depicting a) the positive ion trajectory towards the center axis while the electrode potential is positive and b) the positive ion trajectory away from the center axis while the electrode potential is negative.

voltage is overlaid with the alternative ac voltage across the rods in the x-z plane, heavier ions follow a stable trajectory. The heavier mass ions will not oscillate as rapidly as lighter ions in the electric field, therefore they tend to feel the average potential across the rods. This means the positive dc voltage tends to gain the most influence over heavier ions focusing the beam of heavy ions toward the z axis [120, 121]. The negative half of the ac cycle has minimal effect on the trajectory of these heavier ions. Conversely, lighter ions will experience more movement due to the ac current cycle causing many to strike the rods eliminating them from the beam of ions [120, 121]. This phenomenon creates a filter based upon the mass to charge ratio of the ions. Ions below a particular mass to charge ratio will follow an unstable trajectory, strike the rods, and be removed from the beam leaving only heavier ions on a stable trajectory toward the detector. The rods in the x-z plane charged with positive dc and variable ac voltages perform a high pass mass filter only allowing ions with a sufficiently high mass to charge ratio to transmit through the mass analyzer (Figure 5A) [120, 121].

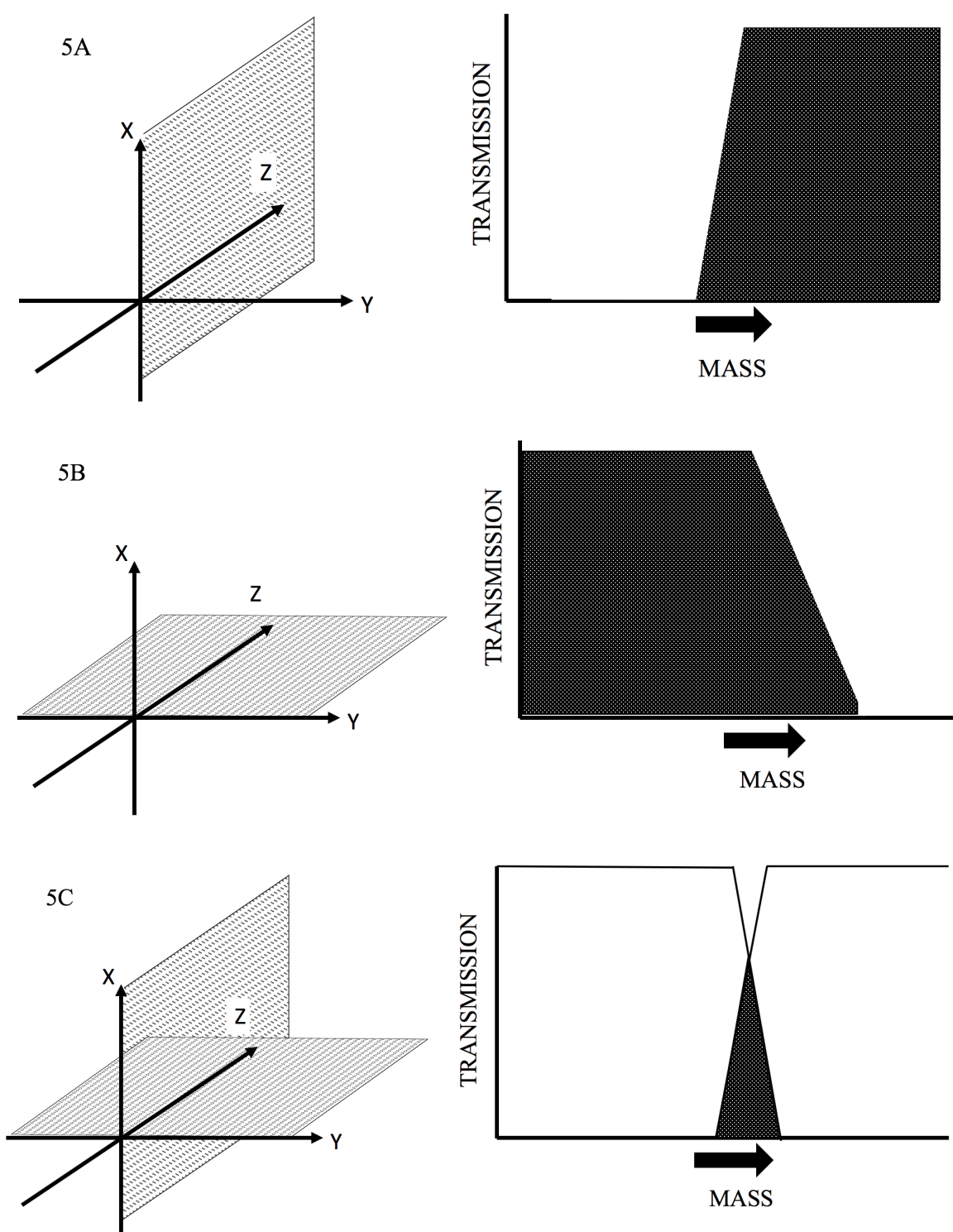


Figure 5: The single quadrupole mass analyzer acting as a mass filter. A) The high mass pass filter created by the quadrupole in the x-z plane. B) The low mass pass filter created by the quadrupole in the y-z plane. C) The combination of the high and low mass pass filters generating the bandpass mass filter.

In the y-z plane, the dc voltage along the pair of rods is equal in magnitude but opposite in sign compared to the rods in the x-z plane. The variable ac voltages applied to the two pairs of rods are arranged 180° out of phase. As in the x-z plane, heavier ions tend to be influenced by the average potential over time. In the y-z plane the dominant influence guiding the heavier ions is the negative dc potential inflicting a defocusing effect drawing these ions away from the z axis causing removal from the beam [120, 121]. The static negative dc potential acts upon lighter ions as well although the positive half of the ac cycle creates a corrective action avoiding elimination from the beam. In the y-z plane the applied negative dc and variable ac potential along the rods performs as a low pass mass filter (Figure 5B) [120, 121].

Ions traveling through this mass analyzer along the z axis follow oscillating trajectories in both x and y directions. In order for an ion to achieve a stable trajectory through the entire mass analyzer it must be sufficiently heavy to pass through the heavy pass filter regulating the x-z plane as well as sufficiently light to pass through the low pass filter regulating the y-z plane. Ions in the mutually stable band representing a select mass to charge ratio will pass through the quadrupole eliminating all other ions (Figure 5C) [120, 121]. The width of the bandpass region is dictated by the ac to dc potentials ratio along the rods akin to the resolution of the instrument. These potentials are kept at a constant ratio but the magnitude of both are fluctuated in order to tune the center of the bandpass region to a desired mass to charge ratio [120, 121].

3.1.4 Photomultiplier Detector

The final stage within the QDa is the photomultiplier detector (Figure 6). The detector contains a photomultiplier tube (PMT), a device amplifying the incident beam of photons or electrons into a cascading flow of photoelectrons striking the detector causing a voltage pulse across a resistor commensurate with the amount of incident particles [126-128]. This technology first emerged in 1935 designed to leverage secondary electron emission within a vacuum phototube amplifying an inbound beam of particles suitable for multiple applications including television and sound movies [129, 130]. The photomultiplier detector is nearly identical to a scintillator counter used for measuring radiation commonly found in handheld survey meters, medical imaging instrumentation, homeland security equipment, as well as mass spectrometry [126, 127, 130-134].

The beam of positive ions exiting the single quadrupole mass analyzer enters the photomultiplier detector (Figure 6). The positive ions strike an oppositely charged electrode ejecting multiple secondary electrons. This electrode, called a dynode, emits electrons when struck by incident ions converting the ion beam into a stream of electrons [128, 135, 136]. These secondary electrons then collide with a phosphorous screen exciting the atoms releasing photons. The photons are directed towards the PMT striking the photocathode connected to the negative terminal of a high voltage source [98, 127, 135, 136]. When struck by the photons, electrons are ejected into the PMT, one electron per photon. The PMT (Figure 7) contains a series of dynodes held at increasingly positive potentials creating an electric field guiding the electrons through the tube striking each dynode [121, 126, 135]. An electron colliding with the first dynode releases multiple secondary electrons which accelerate toward the second dynode. More secondary

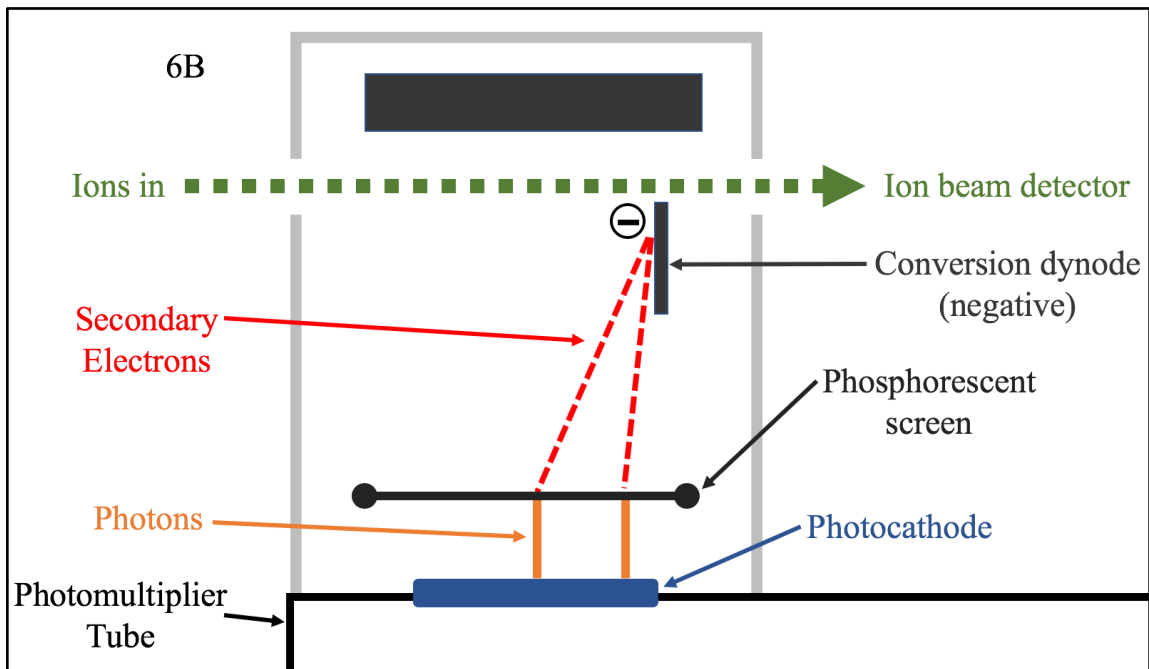
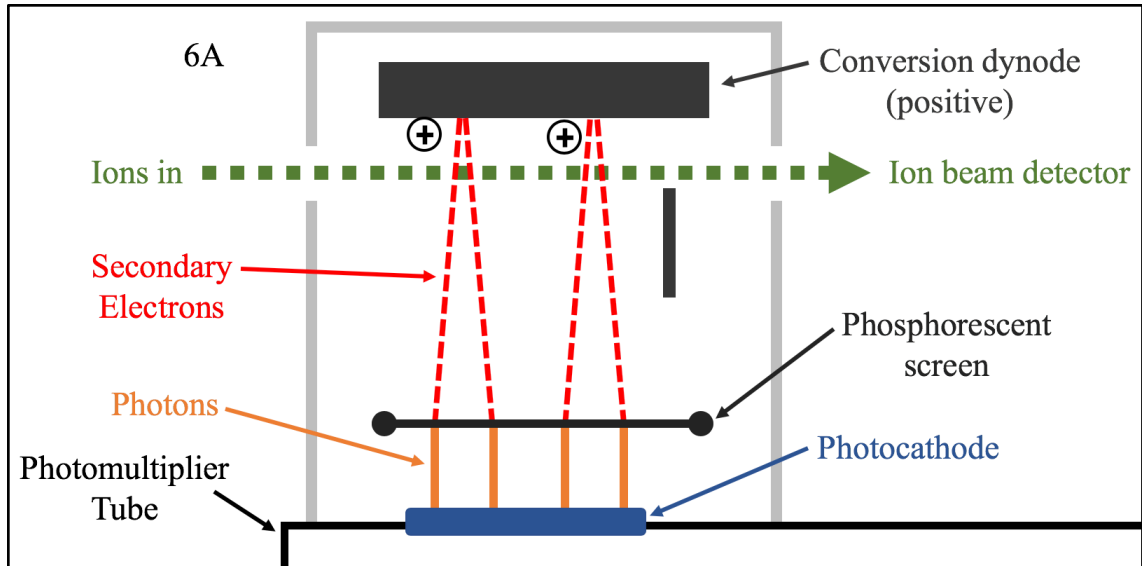


Figure 6: Schematic of a photomultiplier detector operating in a) positive mode and b) negative mode. The stream of ions enters the photomultiplier detector striking the conversion dynode releasing secondary electrons which collide with a phosphorescent screen. This collision releases photons that strike the photocathode of the photomultiplier tube (Figure 7).

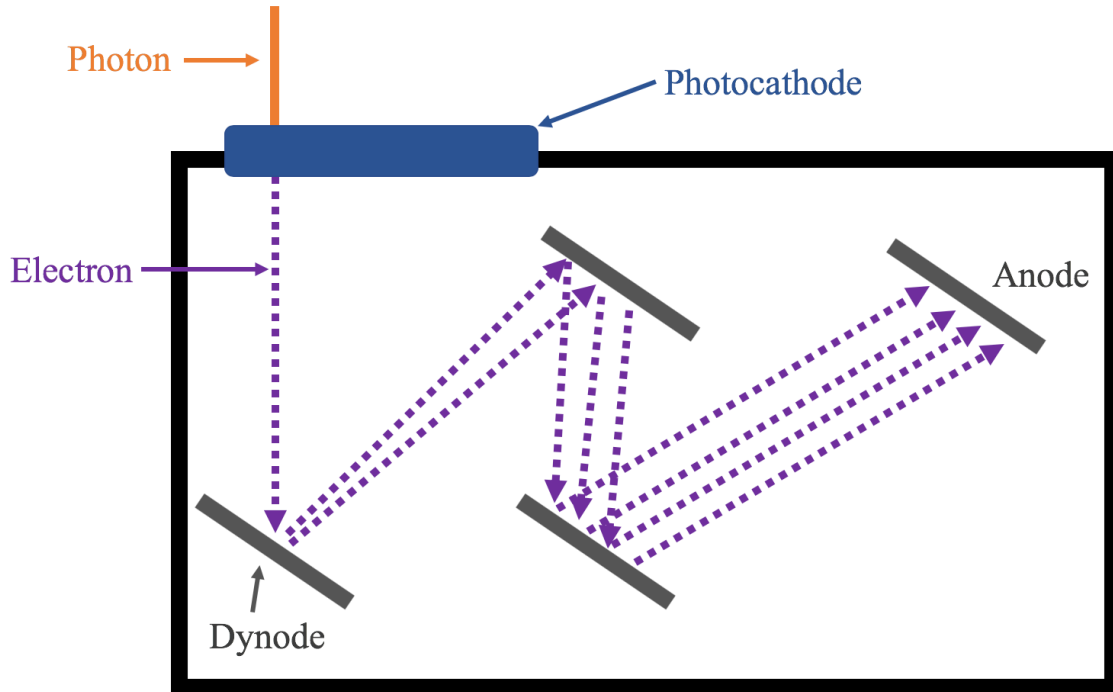


Figure 7: Schematic of a photomultiplier tube (PMT). The photons seen in Figure 6 collide with the photocathode releasing an electron into the PMT. These electrons strike the first dynode initiating a cascade of electrons streaming from dynode to dynode. The series of dynodes contain increasingly positive potentials causing the flow of electrons towards the anode. The electrons end up striking the anode creating a detectable change in voltage.

electrons are released when the second dynode is pummeled by the electrons creating a cascade of electrons significantly amplifying the original signal from the incident beam [127, 128, 135]. A PMT will typically contain ten or more dynodes. This torrent of electrons reaches the anode causing a pulse in the voltage held across resistors measured as the signal corresponding to the amount of initial ions (Figure 7) [98, 126, 127, 135]. This detector operates similarly to an electron multiplier yet avoids the issue of surface contamination on the photocathode by striking the surface with photons instead of particles [98, 135, 136]. For this study, mainly positive mode was used, but negative mode is available using the second dynode within the detector (Figure 6) [128, 135, 136].

The photomultiplier eliminates contamination and is held in a vacuum environment extending the lifetime while providing a rapid, highly sensitive, and robust detector capable of being miniaturized for implementation inside portable instrumentation [98, 127, 128, 135].

3.2 Procedure

The following protocol outlines the procedure completed for rapid, high-throughput analysis of 11 APIs that include: amoxicillin (A) & clavulanic acid (CA), artemether (AM) & lumefantrine (LM), artesunate (ART), azithromycin (AZITH), dihydroartemisinin (DHA) & piperazine (P), ofloxacin (OFLO), and sulfamethoxazole (SM) & trimethoprim (TM). Eight of these APIs are co-formulated combinations inside medicines creating 7 different pharmaceutical treatments evaluated in this study. The standards of these APIs were purchased from TCI Chemical (A, AM, LM, ART, AZITH, DHA, OFLO, SM, and TM), Sigma Aldrich (CA), and Alfa Aesar (P). This study evaluated a series of genuine, substandard, and falsified medicines for every API or API combination. For each API or API combination, between 1 and 4 field collected good quality (FCGQ) medicine(s) were evaluated along with 9 field collected falsified medicines tested for AMLM and 1 tested for SMTM. The majority of the medicines employed in this study were simulated tablets manufactured in the lab across all three classifications: genuine, substandard, and falsified. Genuine medicines created in the lab mimicked the API concentrations and excipient ratios exactly. The simulated medicines created in the lab included 3 with 80% of the correct API concentration and 3 with 50% of the correct API concentration along with a common excipient mixed into the tablet.

The 3 common excipients used across all medicine classifications included lactose, cellulose, and starch all from Sigma Aldrich. The 6 simulated falsified medicines created in house included 3 containing an incorrect API, acetaminophen, one excipient, and 0% of the API concentration while the other 3 consisted of pure excipient. Every API or API combination was tested across all classifications and origins including genuine (FCGQ and simulated), substandard (simulated), and falsified (simulated and field collected when available).

The protocol included sample and standards preparation, QDa set-up, and the data analysis methodology (Figure 8). The software MassLynx 4.0 employed in conjunction with the QDa facilitated settings configuration, data collection and processing. The specific details and settings pertaining to each API or API combination are listed in Table 1. This protocol contains the extraction steps adopted from the GPHF Minilab [48] and can be conducted using the materials and measuring devices contained within the “lab-in-a-suitcase” [46, 137].

The sample preparation began with weighing and crushing the pill in aluminum foil or weigh paper. The extraction solution was made with a portion of the pill and the appropriate solution (Table 1). This was followed by the creation of dilution 1 and 2 solutions in succession according to the specifications in Table 1. The target concentration is the concentration a good quality medicine, 100% API concentration, will attain following this protocol. The sample aliquots were drawn from the dilution 2 solutions and injected into the QDa through the six-port injector. The standards used to create the calibration curve followed the same protocol as the corresponding samples for the extraction and dilution 1 solutions. Calibration standards prepared from dilution 1

Table 1. Experimental parameters for each API or API combination. Specific concentrations for the extractions and dilutions can be found in Appendix A.1. The following settings remained the same throughout all experimental runs: detector gain = 10; sampling frequency = 2 Hz; actual frequency = 2 Hz; sample loop = 20 μ L; source temperature = 120 $^{\circ}$ C; flow rate = 0.30 mL/min.

Parameter	Amoxicillin & Clavulanic Acid	Artemether & Lumefantrine	Artesunate	Azithromycin	Dihydroartemisinin & Piperaquine	Ofloxacin	Sulfamethoxazole & Trimethoprim
Mass Spec Settings	ESI - mode Probe T: 500 $^{\circ}$ C ESI Capillary Volt: -0.8 kV Cone Volt: -5V	ESI + mode Probe T: 500 $^{\circ}$ C ESI Capillary Volt: 1.5 kV Cone Volt: 10V	ESI + mode Probe T: 500 $^{\circ}$ C ESI Capillary Volt: 1.5 kV Cone Volt: 10V	ESI + mode Probe T: 500 $^{\circ}$ C ESI Capillary Volt: 1.5 kV Cone Volt: 10V	ESI + mode Probe T: 500 $^{\circ}$ C ESI Capillary Volt: 1.5 kV Cone Volt: 10V	ESI + mode Probe T: 400 $^{\circ}$ C ESI Capillary Volt: 1.4 kV Cone Volt: 10V	ESI + mode Probe T: 400 $^{\circ}$ C ESI Capillary Volt: 1.4 kV Cone Volt: 10V
Single Ion Recording (SIR) Mode (m/z)	A: 364.00 [M-H] ⁻ CA: 198.10 [M-H] ⁻	AM: 321.16 [M+Na] ⁺ LM: 528.16 [M+H] ⁺	407.30 [M+Na] ⁺	375.26 [M+2H] ²⁺	DHA: 307.15 [M+Na] ⁺ P: 268.76 [M+2H] ²⁺	362.10 [M+H] ⁺	SM: 254.06 [M+H] ⁺ TM: 291.15 [M+H] ⁺
Concentration Range (ppm)	A: 0.85 - 7.01 CA: 0.15 - 0.99	AM: 0.01 - 0.1 LM: 0.6 - 6	0.1 - 1	0.1 - 1	DHA: 0.01 - 0.1 P: 1 - 3	0.1 - 1	SM: 0.5 - 2.5 TM: 0.1 - 0.5
Extraction Solution	H ₂ O	9:1 MeOH:Acetic Acid	MeOH	MeOH	DHA: MeOH P: 99:1 MeOH:HCl	98:2 H ₂ O:Acetic Acid	MeOH
Dilution Solution / Mobile Phase	20:80 H ₂ O:MeOH 2mM Ammonium Acetate	20:80:0.1 H ₂ O:MeOH:Acetic Acid	80:20:0.1 H ₂ O:MeOH:Acetic Acid	80:20:0.1 H ₂ O:MeOH:Acetic Acid	20:80:0.1 H ₂ O:MeOH:Acetic Acid	80:20:0.1 H ₂ O:MeOH:Acetic Acid	80:20:0.1 H ₂ O:MeOH:Acetic Acid
Target Concentration (ppm)	A: 4 CA: 0.285	AM: 0.7 LM: 4.2	0.5	0.5	DHA: 0.05 P: 2	0.5	SM: 1.5 TM: 0.3

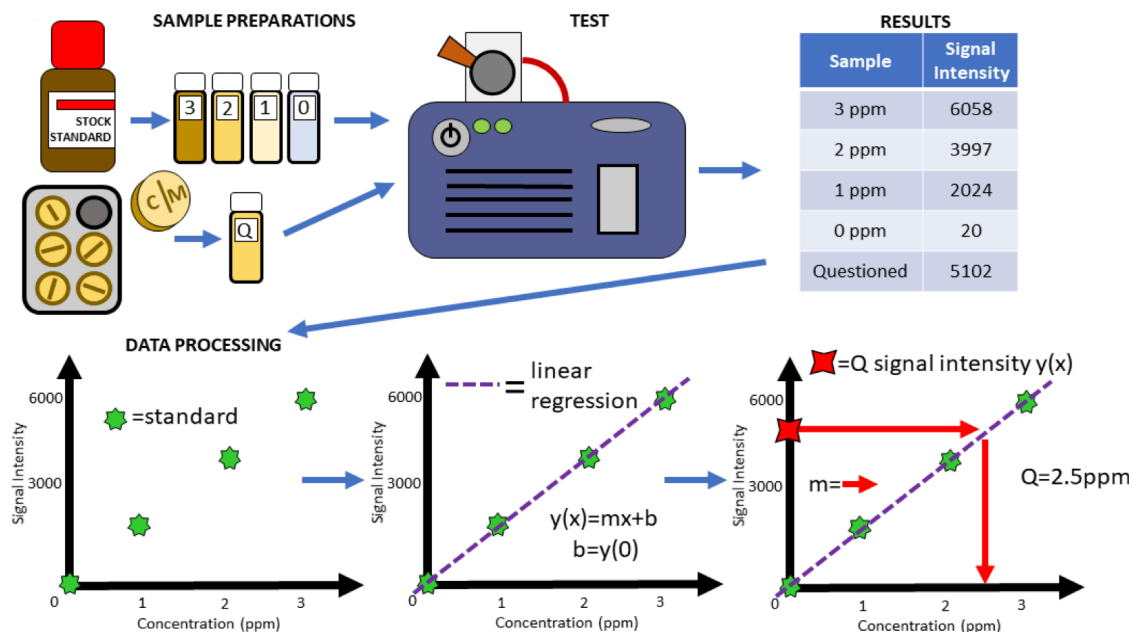


Figure 8: Protocol for QDa experiments. Stock standards were used to create calibration standards while medicines were crushed, extracted and diluted for testing. The signal intensity or abundance was recorded and plotted. The medicine concentration was determined using the linear regression line calculated using the calibration standards.

covered the expanse of the concentration range ideally with two calibration standards above and below the target concentration along with an optional fifth calibration standard at the target concentration.

The QDa set-up began with completing the internal calibration. This instrument allows for internal or external calibration upon initial startup with internal calibration employed in this study. In the MassLynx 4.0 software, specific MS method settings files corresponding to each API and API combination loaded established parameters (Table 1) guiding the flow of ions from sample injection through detection and accumulation of ion counts or abundances.

The experimental runs began with the calibration standards introduced in succession from lowest to highest concentration injected in triplicate allowing the signal

to reliably reach the background between injections. An aliquot of the mobile phase injected in between standards cleaned the sample loop eliminating contamination between standards. After calibration, questioned samples were inserted in the same triplicate manner followed by an aliquot of the mobile phase. The data recorded during each experimental run contained the single ion recording (SIR) chromatogram for each preselected m/z value (Table 1). The resulting chromatogram displayed the ion counts or abundance at the specified m/z value(s) from each injection as a peak (Figure 9).

The data analysis conducted using the chromatogram started by smoothing the data. The chromatogram depicted a series of peaks each corresponding to an injection of calibration standard or sample (Figure 9). The area under each peak corresponded to the abundance of the ions at the specified mass to charge ratio within the injection. A calibration curve created from the calibration standard abundances used the linear regression model producing an equation. The abundances of suspect samples were entered into the linear regression equation calculating a concentration value. This output concentration value was compared with the target concentration to calculate the difference reflected as a percentage. The sample must yield a concentration within 10% of the target concentration for a medicine tablet to be declared good quality. If a sample is outside the $\pm 10\%$ window, the medicine is determined to be poor-quality. This $\pm 10\%$ passing benchmark was adopted from the United States Pharmacopeia (USP) definitions using HPLC in quantifying multiple APIs employed in this study [138, 139]. A medicine was considered a pass if 2/3 injections of the API(s) passed. In a binary co-formulation, 2/3 of both API injections must pass for the medicine to be determined genuine. If 2/3 injections of the API(s) fail, then the medicine was determined to be poor-quality. The

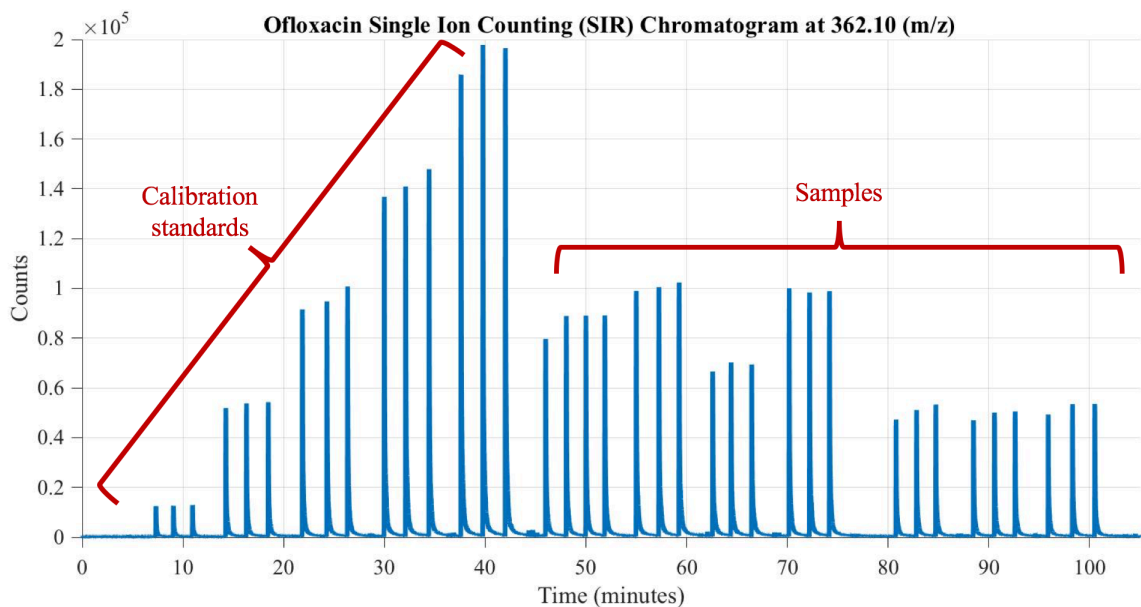


Figure 9: Single ion recording (SIR) mode chromatogram for an ofloxacin experimental run. The run began with the calibration standards followed by the samples all injected in triplicate. The integration of a peak corresponded to the abundance of ions in that injection.

testing and analysis of all medicines proceeded through this protocol with results displayed and discussed in the following chapter.

CHAPTER 4

RESULTS AND DISCUSSION

4.1 Total Ion Current (TIC) mode versus Single Ion Recording (SIR) mode

At the onset of the method development stage, each experiment employed the total ion current (TIC) mode for recording the abundances. In TIC mode, the voltages within single quadrupole mass analyzer rapidly fluctuate sweeping the bandpass filter through a large range of mass to charge ratios (Figure 5). This sweeping action is described as scanning through a predetermined range of mass to charge ratios collecting abundances of ions across the range. The quadrupole will only allow ions of a single mass to charge ratio to traverse through during a fraction of the total time. While employing TIC in experiments, the linear regression calculations revealed adequate but the coefficients of determination (R^2) were not optimal (Figure 10). TIC offers the ability to sweep across a large range in order to determine the dominant analyte species and identify potential contaminants in the sample. Single ion recording (SIR) mode centers the bandpass filter on a single mass to charge ratio for the entirety of the experimental run. This keeps the mass analyzer electronics set to allow ions of the specified mass to charge ratio to traverse on to the detector. The linear regression calculations revealed excellent linearity values increasing the robustness of the data with greater precision and accuracy (Figure 10). The average relative standard deviation (RSD) across the calibration curve for the TIC run was 13.6% while the SIR mode run displayed an RSD of 2.4%. This improvement became crucial when evaluating medicine samples because

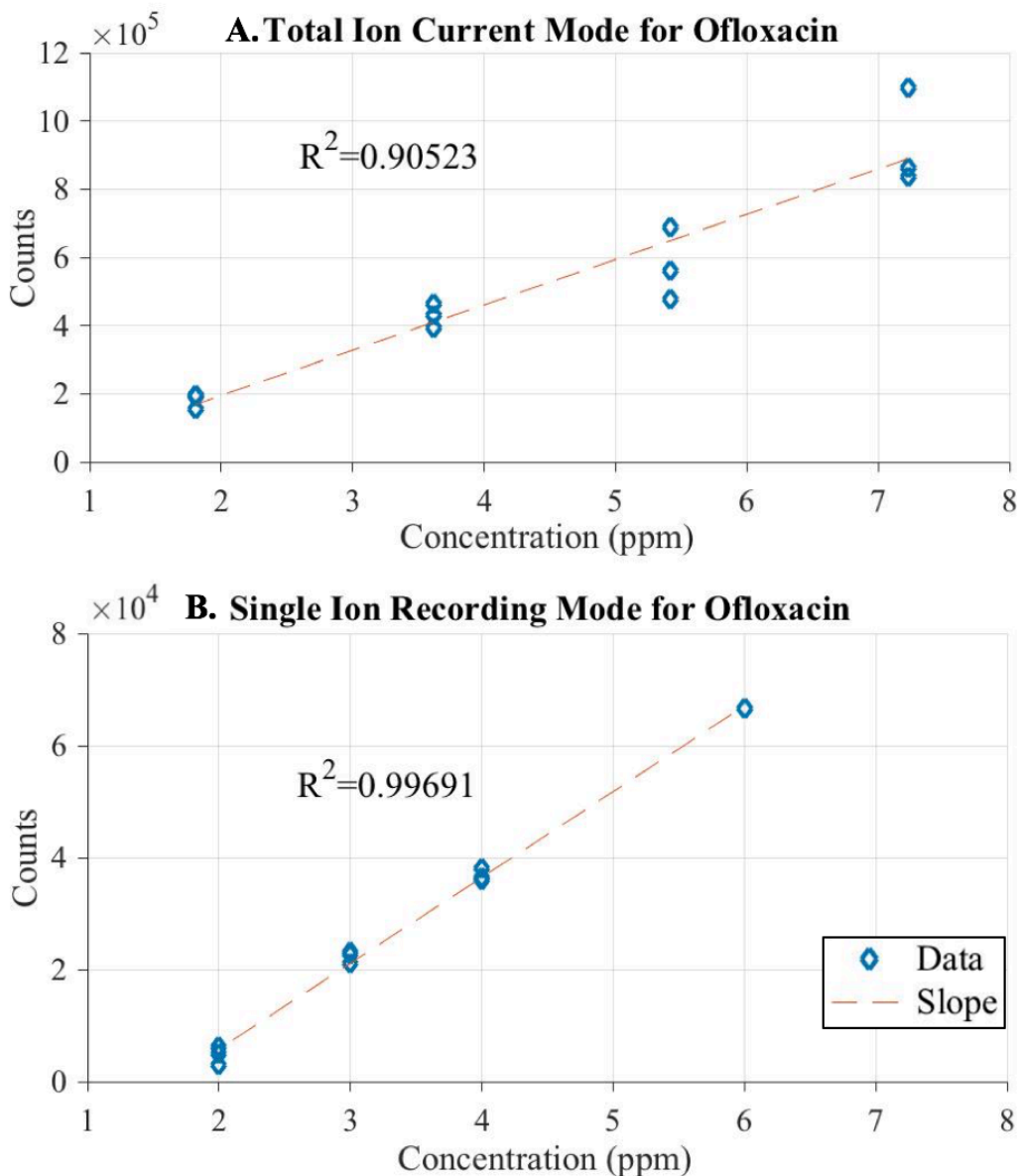


Figure 10: Experimental runs employing identical parameters using a) total ion current (TIC) mode and b) single ion recording (SIR) mode. The linear regression calculations determined the linearity of each line displayed as the R^2 value with the SIR mode achieving higher quality data across all the APIs as illustrated above.

of the tight $\pm 10\%$ window to be declared a pass. SIR mode became the established setting across all APIs for experimental runs. TIC mode could be employed in order to determine the dominant species as well as find impurities.

4.2 Sample Results

The goal of this study was to evaluate the ability of the QDa to perform rapid, high-throughput analysis of poor-quality medicines. The specificity and sensitivity results of this study are summarized in Table 2. The specific results for every medicine tested are listed in Appendix A.1. A total of 123 samples were analyzed across three domains of medicine: genuine, falsified and substandard. The sensitivity and specificity calculations were completed using the true-positive, true-negative, false-positive, and false-negative values [49, 140]. A true-positive is a poor-quality medicine determined to be poor-quality by the instrument. A true-negative is a genuine medicine determined to be genuine by the instrument. A false-positive is a genuine medicine determined to be poor-quality by the instrument. Finally, a false-negative is a poor-quality medicine determined to be genuine by the instrument. Ideally, an instrument would have only true-positives and true-negatives without any false-positives or false-negatives. In this study, the QDa determined 95 true-positives, 21 true-negatives, 7 false-positives, and 0 false-negatives. The binomial specificity and sensitivity calculations incorporated these values.

QDa Sensitivity and Specificity Calculations			
Genuine (n=28) Specificity (95% CI)	Falsified (n=53) Sensitivity (95% CI)	Substandard (n=42) Sensitivity (95% CI)	All PQMs (n=95) Sensitivity (95% CI)
75 (55.1-89.3)	100 (93.3-100)	100 (91.6-100)	100 (96.2-100)

Table 2: The QDa sensitivity and specificity calculations from this study using 123 samples across three classes of medicines: genuine, falsified, and substandard. The binomial calculations employed a 95% confidence interval (CI) shown in the parentheses.

The specificity when analyzing genuine medicines was 75% (55.1-89.3) with a 95% confidence interval (CI). This includes FCGQ and tablets created in the lab. The QDa displayed a competitive specificity compared to other techniques [42, 44, 53, 54] while holding a strict $\pm 10\%$ passing standard. If desired, further testing could establish a unique QDa passing standard potentially allowing greater specificity without compromising the sensitivities. The QDa proved considerably effective in filtering out all poor-quality medicines. The sensitivities of both falsified and substandard medicines were 100% (93.3-100) and 100% (91.6-100), respectively, combining to demonstrate a sensitivity of 100% (96.2-100) when evaluating poor-quality medicines. Studies rarely analyzed separate categories of poor-quality medicines especially in double digit quantities revealing moderate falsified sensitivities yet limited success with substandard sensitivities. Common portable devices have identified falsified medicines evaluating a few APIs [44, 53] yet the lack of breadth and depth in testing antimalarial and antibiotic medicines remains. Substandard medicines continue to plague patients with portable devices unable to differentiate them. The ability of the QDa to characterize substandard medicines from genuine and falsified medicines provides a potential solution for this problem. In this study, the QDa determined 0 false-negatives allowing none of the poor-quality medicines to infiltrate the pool of genuine medicines. The successful results from this device demonstrate the capability of the QDa to potentially become a pivotal instrument in the fight against poor-quality medicines.

Representative calibration curves of ofloxacin, azithromycin and on co-formulated medicine, sulfamethoxazole and trimethoprim, are displayed in Figure 11. The linear regression calculations determined the coefficients of determination (R^2).

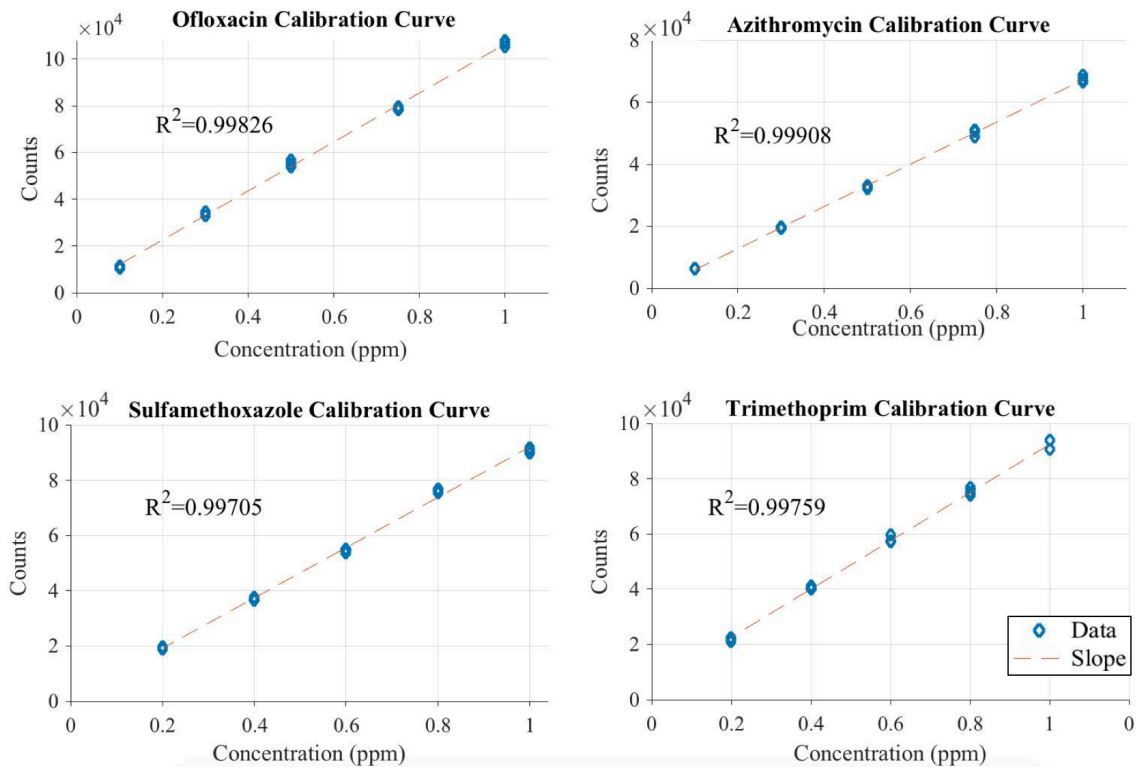


Figure 11: Calibration curves for OFLO, AZITH and one co-formulated combination of SM and TM with the concentration along the x-axis and the abundances displayed as ion counts along the y-axis with the linear fit (R^2) value from the linear regression calculations.

These values being close to 1 demonstrated the calibration standards were within a suitable linear range for each API. The equations produced from the linear regression calculations were used to determine the concentration of each sample injection.

Representative calibration curves for the rest of the APIs are in Appendix A.2.

4.3 Advantages

The QDa presented multiple advantages compared to the current portable devices. First, this device demonstrated a robust capability to separate poor-quality from genuine and falsified from substandard medicines, as revealed by the unprecedented sensitivities.

By employing specific definitions and evaluating both falsified and substandard medicines, the QDa displayed greater in-depth analysis of poor-quality medicines than previous devices. The satisfactory specificity of this device displayed the ability of the QDa to identify genuine medicines comparable to other portable devices while holding to strict passing standard and those studies mostly tested a smaller sample size. This study employed more APIs with more samples than typical device evaluations and conducted more in-depth poor-quality medicine distinctions [44]. The numerous APIs employed in this study encompassed many common antimalarials and antibiotics, some not yet tested with portable devices with the QDa showing strong potential to analyze even more. The rapid, high-throughput capability of the QDa makes it an asset in the continued fight against poor-quality medicines.

This device employs mass spectrometry a widely recognized, robust technique capable of identifying and quantitating analyte APIs, recognizing contaminant APIs, and producing a specific chemical fingerprint [75]. The current set-up of the QDa provides an efficient, sensitive, and durable instrument from ionization source through the detector [75, 84, 120, 136]. This instrument is designed to swiftly analyze various types of molecules within the 30-1250 mass to charge range with limited fragmentation [76, 84]. By utilizing mass spectrometry, the QDa provides thorough compositional analysis to decipher between genuine, falsified and substandard medicines. This instrument is light weight (65 lbs) and low cost (US\$ 75,000) in relation to laboratory mass spectrometers with the start-up cost comparable to some portable spectrometers [44]. The start-up cost although steep for the developing world will acquire an effective device for medicine quality assurance.

Training this technique would be comparable to other techniques. The sample preparation is one additional step to the Minilab protocol [137] utilizing similar reagents and supplies [48, 49, 137]. Methods for the API and API combinations used in this study would serve as a spring board for future implementation with the ability to add other APIs following similar preparation and parameter settings. The user-friendly data analysis software allows for in-depth compositional analysis without requiring in-depth knowledge of data manipulation. Veteran technicians familiar with the protocol and data analysis could incorporate new medicines expanding the analysis portfolio. Implementing the QDa in the field would enable technicians to evaluate the quality of medicines throughout the supply chain discovering crucial intelligence in the fight against poor-quality medicines.

4.4 Disadvantages

The results reveal the QDa is capable of aiding the fight against poor-quality medicines although issues stem from the resources needed and requirements to run the instrument. The largest obstacle to implementing the QDa is the start-up cost. The instrument is US\$ 75,000 also requiring a solvent pump, liquid nitrogen dewars, as well as laboratory grade reagents, glassware, and scales. The steep initial cost pays off as the QDa provides more in-depth analysis compared to other portable techniques some of which also carry a large initial cost. The cost of reagents, glassware and scales from regular use of the instrument is manageable. Routine cleaning and maintenance of the instrument requires additional training, parts, cleaning solvents, and time. If additional

issues requiring maintenance arise then professional help would need to be made available either virtually or in person.

The training and expertise needed for operating the instrument is higher compared to other techniques. Mass spectrometry is highly sensitive but requires delicate and precise preparation and execution to avoid contamination. Various techniques require little to no sample preparation whereas the QDa requires detailed and specific sample preparation increasing the time needed for sample throughput. Troubleshooting issues with the QDa could cause difficulty due to the increased level of mechanical and experimental complexity of the instrument.

An additional significant obstacle is the nitrogen supply required as the desolvation gas for the instrument. The cost and consistent supply of nitrogen will be prohibitive in many places around the world. Also, the QDa requires a stable power supply in order to operate. An unstable power supply would cause trouble in operating the QDa. The necessary supply of nitrogen and power will limit the spread of the QDa inhibiting use in more rural and remote locations where other portable techniques can reach. The opportunity remains for the QDa to reach further into the developing world than current highly sensitive techniques enabling comprehensive, expedient medicine quality assurance testing where previously absent.

In this study, the QDa demonstrated the ability to conduct high-throughput analysis of poor-quality medicines. The practical aspects of the QDa including the initial cost, continuous supply of reagents, and necessary nitrogen and power requirements would need to be addressed for the QDa to reach the portability of other techniques.

4.5 Conclusions

Poor-quality medicines inflict a devastating toll on healthcare systems especially in the developing world. These medicines wreak havoc by robbing patients of treatment and causing further health issues creating a loss of confidence in the health system. The use of these medicines opens an opportunity for drug resistance to flourish. Studies seeking key information on the pervasiveness of the issue yield only glimpses into the multifaceted, devastating situation worldwide. The full extent, consequences, and complexity of the problem continues to be unknown.

Portable devices designed to address this issue bring proven analytical techniques into the field. Highly sensitive techniques rendering detailed compositional information have yet to be converted into a portable device capable of rapid analysis. Portable devices undergoing evaluation have overall demonstrated moderate success in identifying falsified and genuine medicines yet lack the quantitative ability to characterize substandard medicines. The QDa displayed respectable success in the specificity of genuine medicines while employing a stringent $\pm 10\%$ pass standard. The unrivaled success of the QDa in demonstrating excellent sensitivities of falsified and substandard medicines forges the case for further testing and implementation in the fight against poor quality medicines. The rapid, high-throughput analysis of medicinal quality illustrated in this study employed a trainable technique using specifically tailored methods for 7 APIs or API combinations. The QDa performed in-depth evaluation of these common antimalarials and antibiotics yielding promising results in an efficient manner. The practical limitations of the QDa prohibit this device from reaching many remote areas that other portable techniques could, yet the information gained in utilizing this device

merits further testing and implementation to locations able to sustain this technique. The QDa therefore garners the classification of semi-portable. Upon further successful testing of the QDa in determining genuine, falsified, and substandard medicines, this device could arm MRAs, authorized manufactures, and others with a formidable tool in the fight against poor-quality medicines.

APPENDIX A.1

QDa Sample Data from all Active Pharmaceutical Ingredients (APIs)

Table 3: The tables below contain the data from medicines containing a) ACA, b) AMLM, c) ART, d) AZITH, e) DHAP, f) OFLO, and g) SMTM. The “sim” stands for simulated medicines created in the laboratory; “LAC” means the excipient is lactose; “CEL” means the excipient is cellulose; “STR” means the excipient is starch; “FC” means a field collected sample; “ND” means not detected indicating no abundances counted above the background due to the injection. The results are a ratio of the calculated concentration compared to the expected concentration of an injection from the target concentration (100% API(s)). All results within $\pm 10\%$ of the target concentration pass (green), all others fail (red). Medicines are considered good quality if the API(s) pass at least two out of three injections.

Table 3A		Amoxicillin Concentration (%)			Clavulanic Acid Concentration (%)		
Sample ID	Sample Type	Injection 1	Injection 2	Injection 3	Injection 1	Injection 2	Injection 3
RC-ACA	Sim 100% APIs	105.2	105.8	100.2	105.7	102.4	99.2
SS80-ACA-LAC	Sim substandard 80% APIs	81.8	81.3	72.8	85.1	89.7	72.3
SS80-ACA-CEL	Sim substandard 80% APIs	83.0	84.9	75.9	84.8	81.9	76.3
SS80-ACA-STR	Sim substandard 80% APIs	90.4	90.7	90.9	88.9	86.8	82.9
SS50-ACA-LAC	Sim substandard 50% APIs	50.3	50.1	46.9	60.8	63.0	55.9
SS50-ACA-CEL	Sim substandard 50% APIs	55.1	55.1	47.1	58.4	57.2	56.2
SS50-ACA-STR	Sim substandard 50% APIs	57.2	57.6	53.1	65.3	60.7	54.4
EX-LAC	Sim falsified 100% excipient	ND	ND	ND	ND	ND	ND
EX-CEL	Sim falsified 100% excipient	ND	ND	ND	ND	ND	ND
EX-STR	Sim falsified 100% excipient	ND	ND	ND	ND	ND	ND
SM-ACET-LAC	Sim falsified Acetaminophen with 0% APIs	ND	ND	ND	ND	ND	ND
SM-ACET-CEL	Sim falsified Acetaminophen with 0% APIs	ND	ND	ND	ND	ND	ND
SM-ACET-STR	Sim falsified Acetaminophen with 0% APIs	ND	ND	ND	ND	ND	ND
Augmentin (G563)	FCGQ	102.0	102.2	94.4	90.0	89.4	82.4
Cavumox (G528)	FCGQ	108.9	109.4	96.8	96.0	99.8	84.5

Table 3B		Artemether Concentration (%)			Lumefantrine Concentration (%)		
Sample ID	Type Of Sample	Injection 1	Injection 2	Injection 3	Injection 1	Injection 2	Injection 3
RC-AMLM	Sim 100% APIs	104.0	102.9	107.9	90.2	87.5	90.1
SS80-AMLM-LAC	Sim substandard 80% APIs	69.3	69.1	71.4	78.7	74.7	73.9
SS80-AMLM-CEL	Sim substandard 80% APIs	67.7	67.9	69.7	76.5	72.0	72.0
SS80-AMLM-STR	Sim substandard 80% APIs	77.1	72.5	72.6	75.4	68.8	69.3
SS50-AMLM-LAC	Sim substandard 50% APIs	38.1	35.2	40.2	47.0	44.2	44.0
SS50-AMLM-CEL	Sim substandard 50% APIs	46.8	42.5	44.2	44.9	41.9	42.1
SS50-AMLM-STR	Sim substandard 50% APIs	58.1	60.5	59.8	46.3	44.1	43.6
EX-LAC	Sim falsified 100% excipient	ND	ND	ND	ND	ND	ND
EX-CEL	Sim falsified 100% excipient	ND	ND	ND	ND	ND	ND
EX-STR	Sim falsified 100% excipient	ND	ND	ND	ND	ND	ND
SM-ACET-LAC	Sim falsified Acetaminophen with 0% APIs	ND	ND	ND	ND	ND	ND
SM-ACET-CEL	Sim falsified Acetaminophen with 0% APIs	ND	ND	ND	ND	ND	ND
SM-ACET-STR	Sim falsified Acetaminophen with 0% APIs	ND	ND	ND	ND	ND	ND
Coartem (K19)	FCGQ	102.8	100.7	105.9	95.6	88.7	89.0
LC15	FC Falsified	ND	ND	ND	ND	ND	ND
LC5	FC Falsified	ND	ND	ND	ND	ND	ND
LC9	FC Falsified	ND	ND	ND	ND	ND	ND
N1	FC Falsified	ND	ND	ND	ND	ND	ND
N15	FC Falsified	ND	ND	ND	ND	ND	ND
N19	FC Falsified	ND	ND	ND	ND	ND	ND
N3	FC Falsified	ND	ND	ND	ND	ND	ND
N34	FC Falsified	ND	ND	ND	ND	ND	ND
N36	FC Falsified	ND	ND	ND	ND	ND	ND
N5	FC Falsified	ND	ND	ND	ND	ND	ND

Table 3C		Artesunate % Concentration		
Sample ID	Type Of Sample	Injection 1	Injection 2	Injection 3
SM-ART	Sim 100% APIs	106.0	110.0	101.9
SS80-ART-LAC	Sim substandard 80% APIs	70.9	68.2	74.8
SS80-ART-CEL	Sim substandard 80% APIs	78.9	80.7	77.3
SS80-ART-STR	Sim substandard 80% APIs	77.9	79.3	80.8
SS50-ART-LAC	Sim substandard 50% APIs	47.4	46.8	47.3
SS50-ART-CEL	Sim substandard 50% APIs	49.9	52.1	51.9
SS50-ART-STR	Sim substandard 50% APIs	69.4	69.2	69.4
EX-LAC	Sim falsified 100% excipient	ND	ND	ND
EX-CEL	Sim falsified 100% excipient	ND	ND	ND
EX-STR	Sim falsified 100% excipient	ND	ND	ND
SM-ACET-LAC	Sim falsified Acetaminophen with 0% APIs	ND	ND	ND
SM-ACET-CEL	Sim falsified Acetaminophen with 0% APIs	ND	ND	ND
SM-ACET-STR	Sim falsified Acetaminophen with 0% APIs	ND	ND	ND
Artesun G548-2	FCGQ	110.1	110.6	109.3

Table 3D		Azithromycin % Concentration		
Sample ID	Type Of Sample	Injection 1	Injection 2	Injection 3
SM-AZITH-LAC	Sim 100% APIs	97.8	101.2	103.4
SM-AZITH-CEL	Sim 100% APIs	90.0	92.8	95.8
SM-AZITH-STR	Sim 100% APIs	92.1	95.0	93.7
SS80-AZITH-LAC	Sim substandard 80% APIs	74.1	83.7	85.7
SS80-AZITH-CEL	Sim substandard 80% APIs	81.4	87.7	85.3
SS80-AZITH-STR	Sim substandard 80% APIs	84.5	80.9	79.1
SS50-AZITH-LAC	Sim substandard 50% APIs	51.8	54.9	55.0
SS50-AZITH-CEL	Sim substandard 50% APIs	47.2	52.1	51.0
SS50-AZITH-STR	Sim substandard 50% APIs	49.4	53.3	51.9
EX-LAC	Sim falsified 100% excipient	ND	ND	ND
EX-CEL	Sim falsified 100% excipient	ND	ND	ND
EX-STR	Sim falsified 100% excipient	ND	ND	ND
SM-ACET-LAC	Sim falsified Acetaminophen with 0% APIs	ND	ND	ND
SM-ACET-CEL	Sim falsified Acetaminophen with 0% APIs	ND	ND	ND
SM-ACET-STR	Sim falsified Acetaminophen with 0% APIs	ND	ND	ND
Oralzicin (LA 17/06)	FCGQ	96.6	96.9	98.1
Azithromax (LA 16/15)	FCGQ	90.9	91.9	89.8

Table 3E		Dihydroartemisinin % Concentration			Piperazine % Concentration		
Sample ID	Type Of Sample	Injection 1	Injection 2	Injection 3	Injection 1	Injection 2	Injection 3
RC-DHAP	Sim 100% APIs	103.7	99.4	103.9	106.8	110.5	106.3
SS80-DHAP-LAC	Sim substandard 80% APIs	52.2	52.9	49.2	88.8	89.7	89.4
SS80-DHAP-CEL	Sim substandard 80% APIs	56.2	54.3	56.2	79.4	80.6	81.0
SS80-DHAP-STR	Sim substandard 80% APIs	53.7	51.1	54.3	88.5	89.1	85.9
SS50-DHAP-LAC	Sim substandard 50% APIs	31.8	30.4	27.6	46.5	47.1	46.1
SS50-DHAP-CEL	Sim substandard 50% APIs	29.7	29.3	31.1	52.2	53.4	58.0
SS50-DHAP-STR	Sim substandard 50% APIs	31.0	31.1	30.5	48.7	48.0	51.0
EX-LAC	Sim falsified 100% excipient	ND	ND	ND	ND	ND	ND
EX-CEL	Sim falsified 100% excipient	ND	ND	ND	ND	ND	ND
EX-STR	Sim falsified 100% excipient	ND	ND	ND	ND	ND	ND
SM-ACET-LAC	Sim falsified Acetaminophen with 0% APIs	ND	ND	ND	ND	ND	ND
SM-ACET-CEL	Sim falsified Acetaminophen with 0% APIs	ND	ND	ND	ND	ND	ND
SM-ACET-STR	Sim falsified Acetaminophen with 0% APIs	ND	ND	ND	ND	ND	ND
D-Artepp (G552-3)	FCGQ	109.8	109.0	111.4	107.0	109.0	110.8

Table 3F		Ofloxacin % Concentration		
Sample ID	Type Of Sample	Injection 1	Injection 2	Injection 3
SM-OFLO-LAC	Sim 100% APIs	95.3	95.9	95.0
SM-OFLO-CEL	Sim 100% APIs	91.1	90.6	84.9
SM-OFLO-STR	Sim 100% APIs	99.6	103.2	103.7
SS80-OFLO-LAC-001	Sim substandard 80% APIs	75.5	76.4	75.6
SS80-OFLO-CEL-001	Sim substandard 80% APIs	80.4	81.6	69.4
SS80-OFLO-STR-001	Sim substandard 80% APIs	82.0	86.5	82.3
SS50-OFLO-LAC-001	Sim substandard 50% APIs	54.3	57.3	58.5
SS50-OFLO-CEL-001	Sim substandard 50% APIs	55.1	56.2	57.7
SS50-OFLO-STR-001	Sim substandard 50% APIs	55.8	60.4	58.2
EX-LAC-001	Sim falsified 100% excipient	ND	ND	ND
EX-CEL-001	Sim falsified 100% excipient	ND	ND	ND
EX-STR-001	Sim falsified 100% excipient	ND	ND	ND
SM-ACET-LAC-001	Sim falsified Acetaminophen with 0% APIs	ND	ND	ND
SM-ACET-CEL-001	Sim falsified Acetaminophen with 0% APIs	ND	ND	ND
SM-ACET-STR-001	Sim falsified Acetaminophen with 0% APIs	ND	ND	ND
Ofloxin 200 (LA 16-122)	FCGQ	95.9	95.8	97.8
Di-Flo 200 (G546)	FCGQ	94.5	96.0	91.6
CDP Ofloxacin (G570)	FCGQ	84.4	86.9	88.2
Oflocee (G569)	FCGQ	105.7	105.2	104.7

Table 3G		Sulfamethoxazole % Concentration			Trimethoprim % Concentration		
Sample ID	Type Of Sample	Injection 1	Injection 2	Injection 3	Injection 1	Injection 2	Injection 3
SM-SMTM-LAC	Sim 100% APIs	97.1	99.9	97.8	92.3	96.0	97.3
SM-SMTM-CEL	Sim 100% APIs	100.1	101.5	106.5	103.7	111.3	113.5
SM-SMTM-STR	Sim 100% APIs	100.8	109.8	112.3	91.5	95.4	103.2
SS80-SMTM-LAC	Sim substandard 80% APIs	79.2	79.2	77.9	89.7	82.7	81.4
SS80-SMTM-CEL	Sim substandard 80% APIs	69.8	69.5	71.8	70.6	74.3	73.0
SS80-SMTM-STR	Sim substandard 80% APIs	68.9	71.9	72.6	72.2	72.8	75.2
SS50-SMTM-LAC	Sim substandard 50% APIs	41.7	43.1	43.1	65.7	66.7	66.1
SS50-SMTM-CEL	Sim substandard 50% APIs	53.1	54.8	52.0	47.9	48.2	45.9
SS50-SMTM-STR	Sim substandard 50% APIs	50.7	50.8	51.3	54.9	53.0	51.5
EX-LAC	Sim falsified 100% excipient	ND	ND	ND	ND	ND	ND
EX-CEL	Sim falsified 100% excipient	ND	ND	ND	ND	ND	ND
EX-STR	Sim falsified 100% excipient	ND	ND	ND	ND	ND	ND
SM-ACET-LAC	Sim falsified Acetaminophen with 0% APIs	ND	ND	ND	ND	ND	ND
SM-ACET-CEL	Sim falsified Acetaminophen with 0% APIs	ND	ND	ND	ND	ND	ND
SM-ACET-STR	Sim falsified Acetaminophen with 0% APIs	ND	ND	ND	ND	ND	ND
Bispetrim (G540)	FCGQ	98.5	97.9	96.5	99.3	104.6	105.4
Sulfatrim (G571)	FCGQ	111.5	116.2	114.9	103.0	105.3	107.7
Strim-side (LA16-70)	FCGQ	100.1	96.9	94.5	98.2	99.4	98.9
Vactrim (G556)	FCGQ	112.4	106.1	110.2	107.2	107.0	107.2
Griseafulvin (LA13-02)	FC Falsified	ND	ND	ND	ND	ND	ND

APPENDIX A.2

Calibration Curves for Amoxicillin, Clavulanic Acid, Artemether, Lumefantrine, Artesunate, Azithromycin, Dihydroartemisinin, and Piperazine

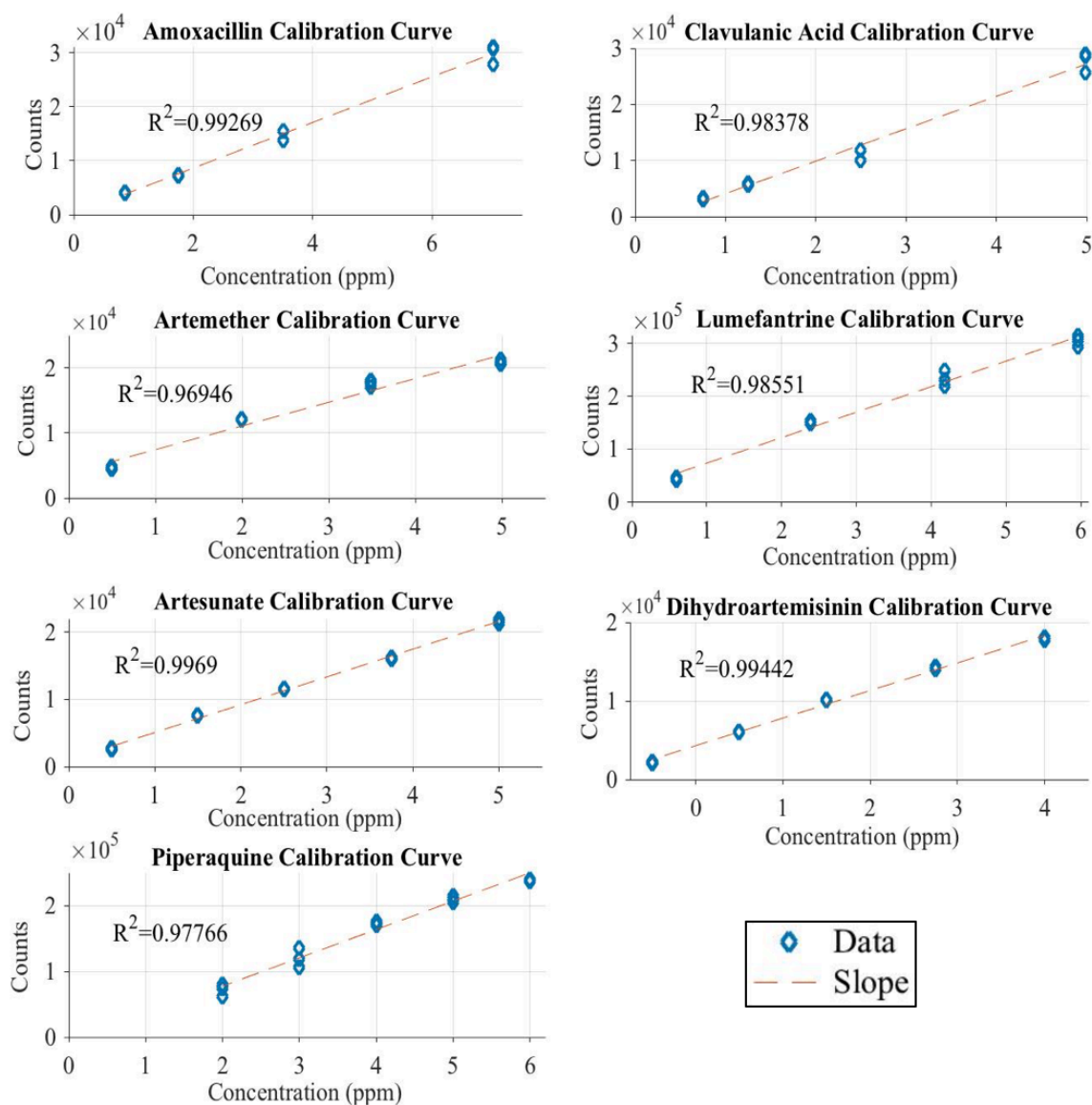


Figure 12: Calibration curves for A, CA, AM, LM, ART, DHA, and P with the concentration along the x-axis and the abundances displayed as ion counts along the y-axis with the linear fit (R^2) value from the linear regression calculations.

REFERENCES

1. Newton, P.N., et al., *Counterfeit anti-infective drugs*. *Lancet Infect Dis*, 2006. **6**(9): p. 602-13.
2. Fernandez, F.M., et al., *Poor quality drugs: grand challenges in high throughput detection, countrywide sampling, and forensics in developing countries*. *Analyst*, 2011. **136**(15): p. 3073-82.
3. Newton, P.N., M.D. Green, and F.M. Fernandez, *Impact of poor-quality medicines in the 'developing' world*. *Trends Pharmacol Sci*, 2010. **31**(3): p. 99-101.
4. Newton, P.N., et al., *The Primacy of Public Health Considerations in Defining Poor Quality Medicines*. *Plos Medicine*, 2011. **8**(12).
5. Newton, P.N., et al., *Guidelines for field surveys of the quality of medicines: a proposal*. *PLoS Med*, 2009. **6**(3): p. e52.
6. World Health Organization. *Substandard and falsified medical products*. 2018 31 January 2018 [cited 2018 11 July]; Available from: <http://www.who.int/en/news-room/fact-sheets/detail/substandard-and-falsified-medical-products>.
7. World Health Organization, *Counterfeit Drugs: Report of a WHO/IFPMA Workshop*. 1992, World Health Organization: Geneva.
8. World Health Organization, *Member State mechanism on substandard/spurious/false-labelled/falsified/counterfeit medical products*. 2017, World Health Organization: Geneva.
9. World Health Organization, *WHO Global Surveillance and Monitoring System for Substandard and Falsified Medical Products*. 2017, World Health Organization: Geneva.
10. World Health Organization, *World Malaria Report 2017*. 2017, Geneva: World Health Organization.
11. Brock, A.R., et al., *The role of antimalarial quality in the emergence and transmission of resistance*. *Med Hypotheses*, 2018. **111**: p. 49-54.
12. World Health Organization, *Malaria: draft global technical strategy: post 2015*. 2015, World Health Organization: Geneva.
13. Murray, C.J., et al., *Global malaria mortality between 1980 and 2010: a systematic analysis*. *Lancet*, 2012. **379**(9814): p. 413-31.

14. Bonelli, R.R., B.M. Moreira, and R.C. Picao, *Antimicrobial resistance among Enterobacteriaceae in South America: History, current dissemination status and associated socioeconomic factors*. Drug Resistance Updates, 2014. **17**(1-2): p. 24-36.
15. Laxminarayan, R., et al., *Access to effective antimicrobials: a worldwide challenge*. Lancet, 2016. **387**(10014): p. 168-75.
16. Liu, L., et al., *Global, regional, and national causes of child mortality in 2000-13, with projections to inform post-2015 priorities: an updated systematic analysis*. Lancet, 2015. **385**(9966): p. 430-40.
17. World Health Organization, *Counterfeit Medicines: an Update on Estimates*. 2006, World Health Organization: Geneva. p. 3.
18. Nayyar, G.M., et al., *Poor-quality antimalarial drugs in southeast Asia and sub-Saharan Africa*. Lancet Infect Dis, 2012. **12**(6): p. 488-96.
19. Group, A.C., et al., *Do anti-malarials in Africa meet quality standards? The market penetration of non quality-assured artemisinin combination therapy in eight African countries*. Malar J, 2017. **16**(1): p. 204.
20. Karunamoorthi, K., *The counterfeit anti-malarial is a crime against humanity: a systematic review of the scientific evidence*. Malar J, 2014. **13**: p. 209.
21. Taberner, P., et al., *Mind the gaps--the epidemiology of poor-quality anti-malarials in the malarious world--analysis of the WorldWide Antimalarial Resistance Network database*. Malar J, 2014. **13**: p. 139.
22. Degardin, K., Y. Roggo, and P. Margot, *Understanding and fighting the medicine counterfeit market*. J Pharm Biomed Anal, 2014. **87**: p. 167-75.
23. Ambroise-Thomas, P., *The tragedy caused by fake antimalarial drugs*. Mediterr J Hematol Infect Dis, 2012. **4**(1): p. e2012027.
24. Grech, J., et al., *An empirical review of antimalarial quality field surveys: the importance of characterising outcomes*. J Pharm Biomed Anal, 2018. **147**: p. 612-623.
25. Attaran, A., R. Bate, and M. Kendall, *Why and how to make an international crime of medicine counterfeiting*. Journal of International Criminal Justice, 2011. **9**(2): p. 325-354.
26. Koczwara, A. and J. Dressman, *Poor-quality and counterfeit drugs: a systematic assessment of prevalence and risks based on data published from 2007 to 2016*. J Pharm Sci, 2017. **106**(10): p. 2921-2929.

27. Almuzaini, T., I. Choonara, and H. Sammons, *Substandard and counterfeit medicines: a systematic review of the literature*. *BMJ Open*, 2013. **3**(8): p. e002923.
28. Newton, P.N., et al., *Poor quality vital anti-malarials in Africa - an urgent neglected public health priority*. *Malar J*, 2011. **10**: p. 352.
29. Mbengue, A., et al., *A molecular mechanism of artemisinin resistance in Plasmodium falciparum malaria*. *Nature*, 2015. **520**(7549): p. 683.
30. Petersen, I., R. Eastman, and M. Lanzer, *Drug-resistant malaria: Molecular mechanisms and implications for public health*. *FEBS letters*, 2011. **585**(11): p. 1551-1562.
31. Menard, D. and A. Dondorp, *Antimalarial Drug Resistance: A Threat to Malaria Elimination*. *Cold Spring Harb Perspect Med*, 2017. **7**(7).
32. White, N.J., et al., *Hyperparasitaemia and low dosing are an important source of anti-malarial drug resistance*. *Malaria Journal*, 2009. **8**(1): p. 253.
33. Newton, P.N., C. Caillet, and P.J. Guerin, *A link between poor quality antimalarials and malaria drug resistance?* 2016, Taylor & Francis.
34. World Health Organization, *Antimicrobial Resistance Key Facts*. 2018, World Health Organization: Geneva.
35. Mackey, T.K., et al., *Counterfeit Drug Penetration into Global Legitimate Medicine Supply Chains: A Global Assessment*. *American Journal of Tropical Medicine and Hygiene*, 2015. **92**(6): p. 59-67.
36. World Health Organization, *Towards Access 2030: WHO Essential Medicines and Health Products Strategic Framework 2016-2030*. 2017, World Health Organization: Geneva.
37. Buckley, G.J., L.O. Gostin, and Institute of Medicine (U.S.). Committee on Understanding the Global Public Health Implications of Substandard Falsified and Counterfeit Medical Products., *Countering the Problem of Falsified and Substandard Drugs*. 2013, Washington, D.C.: THE NATIONAL ACADEMIES PRESS. xxiv, 351 pages.
38. World Health Organization, *Substandard/Spurious/Falsely-Labelled/Falsified/Counterfeit Medical Products*. 2011, World Health Organization: Geneva.
39. Hajjou, M., et al., *Assessment of the performance of a handheld Raman device for potential use as a screening tool in evaluating medicines quality*. *J Pharm Biomed Anal*, 2013. **74**: p. 47-55.

40. Stephen C. Zambrzycki, C.C., Serena Vickers, David V. Donndelinger, Laura C. Winalski, Marcos Bouza, William R. Griggers, Matthew C. Bernier, Paul N. Newton, Facundo M. Fernández, *Evaluation of Thirteen Different Field-deployable Instruments and Low-Cost Technologies for the Detection of Poor-Quality Medicines*. Manuscript in preparation.
41. Yong, Y.L., et al., *Collaborative health and enforcement operations on the quality of antimalarials and antibiotics in southeast Asia*. *Am J Trop Med Hyg*, 2015. **92**(6 Suppl): p. 105-112.
42. Rebiere, H., et al., *Fighting falsified medicines: The analytical approach*. *J Pharm Biomed Anal*, 2017. **142**: p. 286-306.
43. Zou, W.B., L.H. Yin, and S.H. Jin, *Advances in rapid drug detection technology*. *J Pharm Biomed Anal*, 2018. **147**: p. 81-88.
44. Vickers, S., et al., *Field detection devices for screening the quality of medicines: a systematic review*. *BMJ Global Health*, 2018. **3**(4): p. e000725.
45. Kovacs, S., et al., *Technologies for detecting falsified and substandard drugs in low and middle-income countries*. *PLoS One*, 2014. **9**(3): p. e90601.
46. Visser, B.J., et al., *Assessing the quality of anti-malarial drugs from Gabonese pharmacies using the MiniLab(R): a field study*. *Malar J*, 2015. **14**: p. 273.
47. Southern Measurement Company. *C-Vue Chromatography*. 2018 [cited 2018 19 July]; Available from: <http://www.c-vuelc.com/>.
48. Global Pharma Health Fund, E.V. *GPHF-Minilab - Fact Sheet*. 2018 [cited 2018 July 20]; Available from: <https://www.gphf.org/en/minilab/index.htm>.
49. Pan, H. and W. Ba-Thein, *Diagnostic Accuracy of Global Pharma Health Fund Minilab in Assessing Pharmacopoeial Quality of Antimicrobials*. *Am J Trop Med Hyg*, 2018. **98**(1): p. 344-348.
50. Khuluza, F., S. Kigera, and L. Heide, *Low Prevalence of Substandard and Falsified Antimalarial and Antibiotic Medicines in Public and Faith-Based Health Facilities of Southern Malawi*. *Am J Trop Med Hyg*, 2017. **96**(5): p. 1124-1135.
51. World Health Organization, *Survey of the quality of selected antimalarial medicines circulating in six countries of sub-Saharan Africa 2011*, World Health Organization: Geneva.
52. Risha, P., et al., *Proficiency testing as a tool to assess the performance of visual TLC quantitation estimates*. *J AOAC Int*, 2006. **89**(5): p. 1300-4.

53. Baston, J.S., Bempong D. K., *Assessment of the effectiveness of the CD3+ tool to detect counterfeit and substandard anti-malarials*. 2016.
54. Karla Degardin, A.G., Yves Roggo, *Comprehensive Study of a Handheld Raman Spectrometer for the Analysis of Counterfeits of Solid-Dosage From Medicines*. Journal of Spectroscopy, 2017.
55. Wilson, B.K., et al., *A New Handheld Device for the Detection of Falsified Medicines: Demonstration on Falsified Artemisinin-Based Therapies from the Field*. Am J Trop Med Hyg, 2017. **96**(5): p. 1117-1123.
56. Guillemain, A., K. Degardin, and Y. Roggo, *Performance of NIR handheld spectrometers for the detection of counterfeit tablets*. Talanta, 2017. **165**: p. 632-640.
57. United States Pharmacopoeial Convention, *USP Technical Review: CBEx*. 2017: Rockville, Maryland.
58. Zontov, Y., et al., *Chemometric aided NIR portable instrument for rapid assessment of medicine quality*. Journal of pharmaceutical and biomedical analysis, 2016. **131**: p. 87-93.
59. Rebiere, H., et al., *Raman chemical imaging for spectroscopic screening and direct quantification of falsified drugs*. J Pharm Biomed Anal, 2018. **148**: p. 316-323.
60. Visser, B.J., et al., *The diagnostic accuracy of the hand-held Raman spectrometer for the identification of anti-malarial drugs*. Malar J, 2016. **15**: p. 160.
61. Damir Sorak , L.H., Sylvia Iwascek , Sedakat Altinpinar , Frank Pfeifer and H.W. Siesler, *New Developments and Applications of Handheld Raman, Mid-Infrared, and Near-Infrared Spectrometers*, *Applied Spectroscopy Reviews*. 2012: p. 83-115.
62. Weaver, A.A., et al., *Paper analytical devices for fast field screening of beta lactam antibiotics and antituberculosis pharmaceuticals*. Anal Chem, 2013. **85**(13): p. 6453-60.
63. Myers, N., *Lab on Paper: Adapting Quantitative Chemical Techniques for use in Low Resource Areas*. 2017.
64. Guo, S., et al., *Rapid evaluation of artesunate quality with a specific monoclonal antibody-based lateral flow dipstick*. Anal Bioanal Chem, 2016. **408**(22): p. 6003-8.
65. Darash, D., *Pharmachk: robust device for counterfeit and substandard medicines screening on developing regions*. 2014.

66. Marini, R.D., et al., *Reliable low-cost capillary electrophoresis device for drug quality control and counterfeit medicines*. J Pharm Biomed Anal, 2010. **53**(5): p. 1278-87.
67. Nguyen, T.A.H., et al., *Simple semi-automated portable capillary electrophoresis instrument with contactless conductivity detection for the determination of beta-agonists in pharmaceutical and pig-feed samples*. Journal of Chromatography A, 2014. **1360**: p. 305-311.
68. Duong, H.A., et al., *Inexpensive and versatile measurement tools using purpose-made capillary electrophoresis devices coupled with contactless conductivity detection: A view from the case study in Vietnam*. Journal of Science-Advanced Materials and Devices, 2016. **1**(3): p. 273-281.
69. Ranieri, N., et al., *Evaluation of a new handheld instrument for the detection of counterfeit artesunate by visual fluorescence comparison*. Am J Trop Med Hyg, 2014. **91**(5): p. 920-4.
70. Green, M.D., et al., *Integration of novel low-cost colorimetric, laser photometric, and visual fluorescent techniques for rapid identification of falsified medicines in resource-poor areas: application to artemether-lumefantrine*. Am J Trop Med Hyg, 2015. **92**(6 Suppl): p. 8-16.
71. Dunn, J.D., et al., *Using a portable ion mobility spectrometer to screen dietary supplements for sibutramine*. Journal of Pharmaceutical and Biomedical Analysis, 2011. **54**(3): p. 469-474.
72. Gryniewicz, C.M., et al., *Detection of undeclared erectile dysfunction drugs and analogues in dietary supplements by ion mobility spectrometry*. Journal of Pharmaceutical and Biomedical Analysis, 2009. **49**(3): p. 601-606.
73. Qin, C., et al., *Quantitative determination of residual active pharmaceutical ingredients and intermediates on equipment surfaces by ion mobility spectrometry*. Journal of Pharmaceutical and Biomedical Analysis, 2010. **51**(1): p. 107-113.
74. Keil, A., et al., *Ambient mass spectrometry with a handheld mass spectrometer at high pressure*. Analytical Chemistry, 2007. **79**(20): p. 7734-7739.
75. Bernier, M.C., et al., *Fingerprinting of falsified artemisinin combination therapies via direct analysis in real time coupled to a compact single quadrupole mass spectrometer*. Analytical Methods, 2016. **8**(36): p. 6616-6624.
76. Corporation., W. *Acquity QDa Mass Detector*. 2018; Available from: http://www.waters.com/waters/en_US/ACQUITY-QDa-Mass-Detector-for-Chromatographic-Analysis/nav.htm?cid=134761404&locale=en_US.

77. D'Hondt, M., et al., *Implementation of a single quad MS detector in routine QC analysis of peptide drugs*. Journal of pharmaceutical analysis, 2016. **6**(1): p. 24-31.
78. Galba, J., et al., *Quantitative analysis of phenylalanine, tyrosine, tryptophan and kynurenine in rat model for tauopathies by ultra-high performance liquid chromatography with fluorescence and mass spectrometry detection*. Journal of pharmaceutical and biomedical analysis, 2016. **117**: p. 85-90.
79. Gao, J., et al., *A novel compact mass detection platform for the open access (OA) environment in drug discovery and early development*. Journal of pharmaceutical and biomedical analysis, 2016. **122**: p. 1-8.
80. Schepens, E., et al., *Rapid confirmation and quantitation of drugs-of-abuse in oral fluid using a low cost, small footprint mass spectrometer*. Forensic Chemistry, 2017. **4**: p. 75-81.
81. Bu, X., et al., *The emergence of low-cost compact mass spectrometry detectors for chromatographic analysis*. TrAC Trends in Analytical Chemistry, 2016. **82**: p. 22-34.
82. Cech, N.B. and C.G. Enke, *Practical implications of some recent studies in electrospray ionization fundamentals*. Mass Spectrometry Reviews, 2001. **20**(6): p. 362-387.
83. Cole, R.B., *Electrospray and MALDI mass spectrometry: fundamentals, instrumentation, practicalities, and biological applications*. 2011: John Wiley & Sons.
84. Kebarle, P. and U.H. Verkerk, *Electrospray: From Ions in Solution to Ions in the Gas Phase, What We Know Now*. Mass Spectrometry Reviews, 2009. **28**(6): p. 898-917.
85. Pramanik, B.N., A.K. Ganguly, and M.L. Gross, *Applied electrospray mass spectrometry: practical spectroscopy series*. Vol. 32. 2002: CRC Press.
86. Gross, J.H., *Mass spectrometry: a textbook*. 2006: Springer Science & Business Media.
87. Watson, J.T. and O.D. Sparkman, *Introduction to mass spectrometry: instrumentation, applications, and strategies for data interpretation*. 2007: John Wiley & Sons.
88. Dole, M., L.L. Mack, and R.L. Hines, *Molecular Beams of Macroions*. Journal of Chemical Physics, 1968. **49**(5): p. 2240-&.
89. Fenn, J.B., et al., *Electrospray Ionization for Mass-Spectrometry of Large Biomolecules*. Science, 1989. **246**(4926): p. 64-71.

90. Smith, R.D., et al., *New developments in biochemical mass spectrometry: electrospray ionization*. Analytical Chemistry, 1990. **62**(9): p. 882-899.
91. Loo, J.A., *Studying noncovalent protein complexes by electrospray ionization mass spectrometry*. Mass spectrometry reviews, 1997. **16**(1): p. 1-23.
92. Bruins, A.P., T.R. Covey, and J.D. Henion, *Ion spray interface for combined liquid chromatography/atmospheric pressure ionization mass spectrometry*. Analytical Chemistry, 1987. **59**(22): p. 2642-2646.
93. Evans, A.M., et al., *Integrated, nontargeted ultrahigh performance liquid chromatography/electrospray ionization tandem mass spectrometry platform for the identification and relative quantification of the small-molecule complement of biological systems*. Analytical chemistry, 2009. **81**(16): p. 6656-6667.
94. Cahill, J.D., et al., *Determination of pharmaceutical compounds in surface-and ground-water samples by solid-phase extraction and high-performance liquid chromatography–electrospray ionization mass spectrometry*. Journal of Chromatography A, 2004. **1041**(1-2): p. 171-180.
95. Zhou, Z., et al., *Simultaneous determination of clozapine, olanzapine, risperidone and quetiapine in plasma by high-performance liquid chromatography–electrospray ionization mass spectrometry*. Journal of Chromatography B, 2004. **802**(2): p. 257-262.
96. Juan, H., Z. Zhiling, and L. Huande, *Simultaneous determination of fluoxetine, citalopram, paroxetine, venlafaxine in plasma by high performance liquid chromatography–electrospray ionization mass spectrometry (HPLC–MS/ESI)*. Journal of Chromatography B, 2005. **820**(1): p. 33-39.
97. Foppe, K.S. and B. Subedi, *Analysis of Illicit Drugs in Wastewater Using High-Performance Liquid Chromatography-Electrospray Ionization-Tandem Mass Spectrometry (HPLC-ESI-MS/MS)*, in *Analysis of Drugs of Abuse*. 2018, Springer. p. 183-191.
98. Siuzdak, G., *Mass spectrometry for biotechnology*. 1996: Elsevier.
99. Taylor, G. and A. McEwan, *The stability of a horizontal fluid interface in a vertical electric field*. Journal of Fluid Mechanics, 1965. **22**(1): p. 1-15.
100. Fernández de La Mora, J., *The fluid dynamics of Taylor cones*. Annu. Rev. Fluid Mech., 2007. **39**: p. 217-243.
101. Taflin, D.C., T.L. Ward, and E.J. Davis, *Electrified droplet fission and the Rayleigh limit*. Langmuir, 1989. **5**(2): p. 376-384.
102. Gomez, A. and K. Tang, *Charge and fission of droplets in electrostatic sprays*. Physics of Fluids, 1994. **6**(1): p. 404-414.

103. Corporeaon., W., *Fundamentals of Mass Spectrometry - Electrospray Ionization*. 2018.
104. Iribarne, J. and B. Thomson, *On the evaporation of small ions from charged droplets*. The Journal of Chemical Physics, 1976. **64**(6): p. 2287-2294.
105. Thomson, B. and J. Iribarne, *Field induced ion evaporation from liquid surfaces at atmospheric pressure*. The Journal of Chemical Physics, 1979. **71**(11): p. 4451-4463.
106. McFadden, W.H., *Techniques of combined gas chromatography/mass spectrometry*. 1973.
107. Gohlke, R.S. and F.W. McLafferty, *Early gas chromatography/mass spectrometry*. Journal of the American Society for Mass Spectrometry, 1993. **4**(5): p. 367-371.
108. Jennings, W., *Qualitative analysis of flavor and fragrance volatiles by glass capillary gas chromatography*. 2012: Elsevier.
109. Arpino, P.J. and G. Guiochon, *LC/Ms coupling*. Analytical chemistry, 1979. **51**(7): p. 682-701.
110. Niessen, W. and A. Tinke, *Liquid chromatography-mass spectrometry. General principles and instrumentation*. Journal of Chromatography-A incl Cumulative Indexes, 1995. **703**(1): p. 37-58.
111. Blakley, C., J. Carmody, and M. Vestal, *Liquid chromatograph-mass spectrometer for analysis of nonvolatile samples*. Analytical Chemistry, 1980. **52**(11): p. 1636-1641.
112. Gray, A.L., *Solid sample introduction by laser ablation for inductively coupled plasma source mass spectrometry*. Analyst, 1985. **110**(5): p. 551-556.
113. Gray, A.L. and A.R. Date, *Inductively coupled plasma source mass spectrometry using continuum flow ion extraction*. Analyst, 1983. **108**(1290): p. 1033-1050.
114. Jarvis, K.E., et al., *Handbook of inductively coupled plasma mass spectrometry*. 1992: Blackie Glasgow.
115. Yost, R. and C. Enke, *Selected ion fragmentation with a tandem quadrupole mass spectrometer*. Journal of the American Chemical Society, 1978. **100**(7): p. 2274-2275.
116. Nesvizhskii, A.I., et al., *A statistical model for identifying proteins by tandem mass spectrometry*. Analytical chemistry, 2003. **75**(17): p. 4646-4658.

117. Craig, R. and R.C. Beavis, *TANDEM: matching proteins with tandem mass spectra*. *Bioinformatics*, 2004. **20**(9): p. 1466-1467.
118. Eng, J.K., A.L. McCormack, and J.R. Yates, *An approach to correlate tandem mass spectral data of peptides with amino acid sequences in a protein database*. *Journal of the American Society for Mass Spectrometry*, 1994. **5**(11): p. 976-989.
119. Yost, R. and C. Enke, *Triple quadrupole mass spectrometry for direct mixture analysis and structure elucidation*. *Analytical chemistry*, 1979. **51**(12): p. 1251-1264.
120. Miller, P.E. and M.B. Denton, *The quadrupole mass filter: basic operating concepts*. *Journal of chemical education*, 1986. **63**(7): p. 617.
121. Skoog, D.A., F.J. Holler, and S.R. Crouch, *Principles of instrumental analysis*. 2017: Cengage learning.
122. Landais, B., et al., *Varying the radio frequency: a new scanning mode for quadrupole analyzers*. *Rapid communications in mass spectrometry*, 1998. **12**(6): p. 302-306.
123. Chernushevich, I.V., A.V. Loboda, and B.A. Thomson, *An introduction to quadrupole-time-of-flight mass spectrometry*. *Journal of mass spectrometry*, 2001. **36**(8): p. 849-865.
124. Dunn, W.B., *Mass spectrometry in systems biology: An introduction*, in *Methods in enzymology*. 2011, Elsevier. p. 15-35.
125. Syed, S., S. Maher, and S. Taylor, *Quadrupole mass filter operation under the influence of magnetic field*. *Journal of Mass Spectrometry*, 2013. **48**(12): p. 1325-1339.
126. Eisaman, M.D., et al., *Invited review article: Single-photon sources and detectors*. *Review of scientific instruments*, 2011. **82**(7): p. 071101.
127. Neetu, K., et al., *A review on mass spectrometry detectors*. *International Research Journal of Pharmacy*, 2012. **3**(10): p. 33-42.
128. Berezovskaya, Y., *Investigation of protein-ion interactions by mass spectrometry and ion mobility mass spectrometry*. 2012.
129. Iams, H. and B. Salzberg, *The secondary emission phototube*. *Proceedings of the Institute of Radio Engineers*, 1935. **23**(1): p. 55-64.
130. Daly, N., *Scintillation type mass spectrometer ion detector*. *Review of Scientific Instruments*, 1960. **31**(3): p. 264-267.

131. Yeom, J.Y., R. Vinke, and C.S. Levin, *Optimizing timing performance of silicon photomultiplier-based scintillation detectors*. *Physics in Medicine & Biology*, 2013. **58**(4): p. 1207.
132. Garutti, E., *Silicon photomultipliers for high energy physics detectors*. *Journal of Instrumentation*, 2011. **6**(10): p. C10003.
133. Bashkurov, V., et al., *Novel scintillation detector design and performance for proton radiography and computed tomography*. *Medical physics*, 2016. **43**(2): p. 664-674.
134. Akimov, Y.K., *Scintillation counters in high energy physics*. 1965.
135. Dyer, S.A., *Wiley survey of instrumentation and measurement*. 2011: John Wiley & Sons.
136. Gates, P.J. *Ion Detectors*. 2014 [cited 2018 September 7]; Available from: <http://www.chm.bris.ac.uk/ms/detectors.xhtml>.
137. Global Pharma Health Fund, E.V. *GPHF-Minilab-Manuals*. 2018 [cited 2018 September 21]; Available from: <https://www.gphf.org/en/minilab/manuals.htm>.
138. United States Pharmacopoeial Convention, *Amoxicillin and Clavulanate Potassium Tablets*, in *USP Monographs*. 2017.
139. United States Pharmacopoeial Convention, *Azithromycin Tablets*, in *USP Monographs*. 2017.
140. Blacksell, S.D., et al., *The comparative accuracy of 8 commercial rapid immunochromatographic assays for the diagnosis of acute dengue virus infection*. *Clinical Infectious Diseases*, 2006. **42**(8): p. 1127-1134.